

VIBFREQ1295: A New Database for Vibrational Frequency Calculations

Juan Camilo Zapata and Laura K. McKemmish*

School of Chemistry, University of New South Wales, 2052, Sydney

E-mail: l.mckemmish@unsw.edu.au

Abstract

High-throughput approaches for producing approximate vibrational spectral data for molecules of astrochemistry interest rely on harmonic frequency calculations using computational quantum chemistry. However, model chemistry recommendations (i.e, a level of theory and basis set pair) for these calculations are not yet available and, thus, thorough benchmarking against comprehensive benchmark databases is needed.

Here, we present a new database for vibrational frequency calculations (VIBFREQ1295) storing 1,295 experimental fundamental frequencies and CCSD(T)(F12*)/cc-pVDZ-F12 *ab initio* harmonic frequencies from 141 molecules. VIBFREQ1295’s experimental data was compiled through a comprehensive review of contemporary experimental data while the *ab initio* data was computed here. The chemical space spanned by the molecules chosen is considered in depth and shown to have good representation of common organic functional groups and vibrational modes.

Scaling factors are routinely used to approximate the effect of anharmonicity and convert computed harmonic frequencies to predicted fundamental frequencies. With our experimental and high-level *ab initio* data, we find that a single global uniform scaling factor of 0.9617(3) results in median differences of 15.9(5) cm⁻¹. Far superior performance with a median difference of 7.5(5) cm⁻¹ can be obtained, however, by using separate scaling factors for three

regions: frequencies less than 1000 cm^{-1} ($\text{SF} = 0.987(1)$), between 1000 and 2000 cm^{-1} ($\text{SF} = 0.9727(6)$) and above 2000 cm^{-1} ($\text{SF} = 0.9564(4)$). This sets a lower bound for the performance that could be reliably obtained using scaling of harmonic frequencies calculations to predict experimental fundamental frequencies.

VIBFREQ1295's most important purpose is to provide a robust database for benchmarking the performance of any vibrational frequency calculations. VIBFREQ1295 data could also be used to train machine-learning models for the prediction of vibrational spectra, and as a reference and data starting point for more detailed spectroscopic modelling of particular molecules. The database can be found as part of the supplemental material for this paper, or in the Harvard DataVerse at <https://doi.org/10.7910/DVN/VLVNU7>.

Introduction

Definitive remote detection of molecular species in different astronomical settings, e.g (exo)planetary atmospheres, relies on the availability of high-resolution spectroscopic data,¹⁻⁷ which is very time-intensive to produce. As a complementary approach, it is likely to be useful to obtain approximate data for the thousands of molecular species of interest astrophysically, e.g. as discussed in Seager et al.⁸ Though this novel approach^{9,10} cannot enable definitive molecular detections, there are nevertheless many anticipated applications of these big data including identification of molecules with strong absorption (that will be easier to detect), recognising potential ambiguities in molecular detections over some spectral windows, understanding the relative congestion of signals at different frequencies, and providing data for machine learning of vibrational frequencies.

An obvious way to produce this approximate vibrational spectral data for thousands of molecules is through harmonic or anharmonic quantum chemistry vibrational frequency calculations, as piloted in Zapata Trujillo et al.¹⁰ However, existing literature, as recently reviewed in Zapata Trujillo and McKemmish,¹¹ does not provide a definitive recommendation for a quantum chemistry methodology, even within the extremely popular harmonic approximation, nor explore the likely errors. These recommendations and error analysis are of interest far beyond the astrochemistry

community (as evidenced by high citation numbers of, for example, Scott and Radom¹²). We note that there has certainly been significant prior work on this topic (reviewed in Zapata Trujillo and McKemmish¹¹) - it is the reliable definitive modern recommendations that are missing. Root-mean-squared errors (RMSE) between experimental and theoretical scaled harmonic frequencies have been computed extensively to compare model chemistry performance¹¹ but conclusions from this collation can only be preliminary as (1) the RMSE metrics cannot be fairly compared across different publications due to differences in the benchmark datasets used; and (2) there is often a lack of data for many important modern model chemistry choices.

The need for a new thorough and comprehensive benchmarking study of model chemistry performance for harmonic frequency calculations is clear,¹¹ but crucially the quality of this study relies on the quality of the experimental database against which theoretical results are compared. A key focus of this paper is to provide such an updated and collated experimental database, which we call VIBFREQ1295. The need for an update is justified initially by the fact that it has been almost thirty years since the most extensive and frequently used database was compiled in Pople et al.¹³ 1064f/122mol (note this is widely known as the F1 set due to its use in Scott and Radom¹²), then in hindsight by the significant number of updates to this original data that were found.

Given that using scaled harmonic frequencies is the most widespread approach to predict experimental fundamental frequencies in quantum chemistry, understanding the inherent errors of the harmonic approximation at very high levels of model chemistry, e.g., CCSD(T)-like calculations, is pivotal for providing directions into less-demanding and routine calculations. For instance, such comparison can allow us to explore how best to quantify the error distribution and occurrence of large outliers in the calculations. Moreover, we can also examine different approaches for the implementation of scaling factors, highlighting errors and expected performance in each case.

In the present paper, we provide a new benchmark database for vibrational frequencies, containing 1,295 experimental fundamental frequencies from 141 organic-like molecules (VIBFREQ1295). The frequencies collated here correspond to the most up-to-date experimental fundamental frequencies for the molecules considered, as recorded by an extensive literature review search. The

uncertainties in the experimental measurements (when available), the symmetry of the vibration, as well as approximate descriptions to the vibrational modes, are also provided for all molecules in the database. To complement the experimental frequencies, we also calculated high-level CCSD(T)(F12*)/cc-pVDZ-F12 *ab initio* harmonic frequencies for all molecules in the database. The reader can access the VIBFREQ1295 database in the supplemental material for this paper, as well as through the Harvard DataVerse platform¹⁴ (<https://doi.org/10.7910/DVN/VLVNU7>).

This paper is organised as follows. In Section we explain the criteria used to select the molecules and frequencies included in the database, and provide a comparison between the newly compiled experimental frequencies and the data from the previous vibrational frequency databases. A detailed analysis into the chemical space and functional groups included into VIBFREQ1295 is presented in Section , with particular interest in the distribution of different vibrational modes in the database. In Section we present the high-level (CCSD(T)(F12*)¹⁵/cc-pVDZ-F12^{16,17}) *ab initio* harmonic frequencies for the molecules together with our analysis in terms of the scaling factor calculation, its implication on the accuracy of the scaled harmonic frequencies, and the expected anharmonicity error. Finally, in Section we summarise our findings, outlining concluding remarks and future directions for this work.

Constructing the Database

Herein, we present a new database for vibrational frequency calculations containing 1,295 experimental fundamental frequencies and high-quality (CCSD(T)(F12*)¹⁵/cc-pVDZ-F12^{16,17}) *ab initio* harmonic frequencies for 141 molecules. Table 1 presents an overview of the molecules considered in the database, showcasing the total number of atoms and experimental frequencies, frequency range covered, and references to the original experimental publications.

VIBFREQ1295 was built upon data collected from six popular vibrational frequency databases available in the literature that have all been previously used to calculate scaling factors, indicating the suitability of the collated molecules for this purpose. Table 2 outlines the databases considered,

Table 1: Summary of molecular species considered into VIBFREQ1295 listing the molecular formula, IUPAC name, total number of atoms and frequencies, the frequency range covered (in cm^{-1}), number of vibrational frequencies, and the references to the original experimental publications per molecule. Cyclic molecules are indicated with *c*– before the molecular formula. Isomeric molecules (except for *cis* and *trans*) are distinguished by an underscore and number after the molecular formula, e.g., C_3H_4 and $\text{C}_3\text{H}_4\text{--}1$. The electronic state for each molecular species is indicated as a superscript in the left-hand side of the molecular formula whenever the electronic state is not a singlet. Only $^1\text{CH}_2$ (singlet state) is explicitly presented in the table to distinguish it from $^3\text{CH}_2$ (triplet state).

Formula	IUPAC Name	#At	Freq. (cm^{-1})	Vib. Freqs.	Refs	Formula	IUPAC Name	#At	Freq. (cm^{-1})	Vib. Freqs.	Refs
AlCl_3	Aluminium chloride	4	616 - 151	6	23	ClNO	Nitrosyl chloride	3	1799 - 331	3	24,25
BH	λ^1 -borane	2	2269 - 2269	1	26	ClNO_2	Chloro nitrite	4	1683 - 370	6	27-31
BH_3CO	Borane carbonyl	6	2456 - 313	12	32-34	^2ClO	Chlorosyl	2	853 - 853	1	35
^2BO	Oxoboron	2	1772 - 1772	1	36	^2CN	Cyano radical	2	2042 - 2042	1	37
<i>c</i> – $\text{C}_2\text{H}_4\text{S}_3$	1,2,4-trithiolane	9	2976 - 82	21	38	CO	Carbon monoxide	2	2169 - 2169	1	39
<i>c</i> – $\text{C}_3\text{H}_3\text{NO}$	1,3-oxazole	8	3160 - 609	18	40,41	CO_2	Carbon dioxide	3	2349 - 667	4	42-43
<i>c</i> – $\text{C}_3\text{H}_3\text{NO}_1$	1,2-oxazole	8	3160 - 591	18	44	COCl_2	Carbonyl dichloride	4	1828 - 301	6	45-48
<i>c</i> – C_3H_6	Cyclopropane	9	3101 - 737	21	49-53	COClF	Carbonyl chloride fluoride	4	1875 - 408	6	54
<i>c</i> – $\text{C}_3\text{H}_4\text{S}$	Thietane	10	2994 - 113	24	38,55	COF_2	Carbonyl difluoride	4	1944 - 581	6	56-58
<i>c</i> – $\text{C}_4\text{H}_4\text{N}_2$	Pyrazine	10	3069 - 350	24	59	CS	Methanidyldynesulfanium	2	1285 - 1285	1	60
<i>c</i> – $\text{C}_4\text{H}_4\text{O}$	Furan	9	3169 - 599	21	61-66	CS_2	Carbon disulfide	3	1535 - 395	4	67-69
<i>c</i> – $\text{C}_4\text{H}_3\text{N}$	1H-pyrrole	10	3530 - 474	24	62,66,70-73	CSCl_2	Thiocarbonyl dichloride	4	1138 - 297	6	74-76
<i>c</i> – $\text{C}_4\text{H}_4\text{O}_2$	1,4-dioxane	14	2970 - 274	36	18	CSF_2	Difluoromethanethione	4	1368 - 417	6	77
<i>c</i> – $\text{C}_4\text{H}_3\text{N}$	Pyridine	11	3094 - 373	27	78	CF_4	Molecular fluorine	2	893 - 893	1	79
<i>c</i> – CH_2N_4	1H-tetrazole	7	3447 - 578	15	80	F_2O	Fluoro hypofluorite	3	928 - 460	3	81-83
C_2Cl_2	1,2-dichloroethyne	4	2234 - 171	7	84,85	F_2SO	Thionyl fluoride	4	1334 - 376	6	86,87
C_2H_2	Acetylene	4	3372 - 612	7	88-90	FCN	Carbononitridic fluoride	3	2318 - 451	4	91-93
$\text{C}_2\text{H}_2\text{O}$	Ketene	5	3165 - 439	9	94-98	H_2CO	Formaldehyde	4	2843 - 1167	6	99,100
$\text{C}_2\text{H}_2\text{O}_2$	Oxaldehyde	6	2844 - 127	12	101-104	H_2O	Water	3	3755 - 1594	3	105,106
$\text{C}_2\text{H}_3\text{Cl}$	Chloroethene	6	3129 - 395	12	107-112	H_2S	Sulfane	3	2628 - 1182	3	113,114
$\text{C}_2\text{H}_3\text{N}$	Acetonitrile	6	3040 - 362	12	115	HCl	Hydrochloric acid	2	2990 - 2990	1	116
$\text{C}_2\text{H}_3\text{N}_1$	Isocyanomethane	6	3013 - 260	12	117-120	HCN	Hydrogen cyanide	3	3311 - 711	4	121
$\text{C}_2\text{H}_3\text{OF}$	Acetyl fluoride	7	3043 - 123	15	122	^2HCO	Formyl radical	3	2434 - 1080	3	123-125
$\text{C}_2\text{H}_4\text{O}$	Acetaldehyde	7	3014 - 143	15	126-130	HNCO	Isocyanic acid	4	3538 - 577	6	131-134
$\text{C}_2\text{H}_4\text{O}_2$	Methyl formate	8	3045 - 130	18	135	HNO	Nitroxyl	3	2683 - 1500	3	136,137
$\text{C}_2\text{H}_4\text{O}_2\text{--}1$	Acetic acid	8	3585 - 93	18	138,139	HNO_3	Nitric acid	5	3550 - 458	9	140-146
$\text{C}_2\text{H}_3\text{F}$	Fluoroethane	8	3000 - 243	18	147	$^2\text{HO}_2$	Hydroperoxy radical	3	3436 - 1097	3	148-150
C_2H_6	Ethane	8	2985 - 289	18	151-155	HOCl	Hypochlorous acid	3	3609 - 724	3	156,157
$\text{C}_2\text{H}_6\text{O}$	Methoxymethane	9	2993 - 198	21	158-160	HOF	Hypofluorous acid	3	3577 - 889	3	161,162
$\text{C}_2\text{H}_6\text{S}$	Methylsulfanylmethane	9	2998 - 175	21	163,164	N_2F_2	(E)-difluorodiazene	4	1522 - 365	6	165
C_2HCl	Chloroethyne	4	3339 - 324	7	166,167	N_2H_4	Hydrazine	6	3398 - 376	12	168-170
C_2HF	Fluoroethyne	4	3356 - 366	7	171	N_2O	Nitrous oxide	3	2223 - 588	4	172-174
C_2N_2	Oxalonitrile	4	2330 - 233	7	175	NCl_2F	Dichlorofluoroamine	4	825 - 274	6	176
$\text{C}_3\text{H}_3\text{Cl}$	3-chloroprop-1-yne	7	3335 - 186	15	177	NClF_2	Chlorodifluoroamine	4	930 - 378	6	178,179
$\text{C}_3\text{H}_3\text{F}$	3-fluoroprop-1-yne	7	3338 - 211	15	177	NF_3	Nitrogen trifluoride	4	1032 - 493	6	180,181
$\text{C}_3\text{H}_3\text{N}$	Acrylonitrile	7	3123 - 228	15	182,183	^3NH	λ^1 -azane	2	3125 - 3125	1	184
C_3H_4	Propa-1,2-diene	7	3085 - 352	15	185-190	NH_3	Amonia	4	3443 - 968	6	191-193
$\text{C}_3\text{H}_4\text{--}1$	Prop-1-yne	7	3335 - 330	15	187,194-199	NHF_2	Difluoroamine	4	3193 - 500	6	200
$\text{C}_3\text{H}_4\text{O}$	Prop-2-enal	8	3103 - 157	18	201-205	$^2\text{NO}_2$	Nitrogen dioxide	3	1616 - 749	3	206
C_3H_6	Prop-1-ene	9	3091 - 189	21	207-211	NSCl	Azanyldiyne(chloro)- λ^4 -sulfane	3	1325 - 271	3	212,213
C_3H_8	propane	11	2976 - 217	27	214-219	NSF	Azanyldiyne(fluoro)- λ^4 -sulfane	3	1372 - 366	3	220
C_3O_2	Carbon suboxide	5	2289 - 60	10	221-227	O_3	Ozone	3	1103 - 700	3	228
C_4H_2	Buta-1,3-diyne	6	3333 - 219	13	229,230	OCS	Carbonyl sulfide	3	2062 - 521	4	231,232
C_4H_6	Buta-1,3-diene	10	3100 - 162	24	233-237	ONF	Nitrosyl fluoride	3	1844 - 519	3	238,239
C_4N_2	Dicyanoacetylene	6	2296 - 107	13	240-243	P_4	Tetraphosphorus	4	600 - 360	6	244
C_6H_8	(3E)-hexa-1,3,5-triene	14	3099 - 90	36	245	PCl_3	Trichlorophosphane	4	504 - 198	6	246
CCl_2F_2	Dichloro(difluoro)methane	5	1161 - 261	9	247-251	PF_3	Trifluorophosphane	4	891 - 347	6	252
CCl_4	Tetrachloromethane	5	793 - 218	9	253-255	^3PH	λ^1 -phosphane	2	2276 - 2276	1	256
CF_4	Tetrafluoromethane	5	1283 - 435	9	257	PH_3	Phosphine	4	2326 - 992	6	258,259
^2CH	Methyldiyne radical	2	2732 - 2732	1	260	PN	Azanyldiynephosphane	2	1323 - 1323	1	261
CH_2Cl_2	Dichloromethane	5	3055 - 281	9	262	S_2	Disulfur	2	725 - 725	1	263
CH_3N_2	Diazomethane	5	3184 - 408	9	264-266	S_2F_2	Fluorosulfanyl thiohypofluorite	4	717 - 182	6	267
CH_2O_2	Formic acid	5	3568 - 626	9	268-272	S_2O	Disulfur monoxide	3	1166 - 380	3	273-275
CH_2S	Thioformaldehyde	4	3024 - 990	6	276-278	SCL_2	Chloro thiohypochlorite	3	528 - 205	3	279
CH_3Cl	Chloromethane	5	3039 - 732	9	280,281	^2SH	λ^1 -sulfane	2	2599 - 2599	1	282
CH_3F	Fluoromethane	5	2998 - 1048	9	283-286	Si_2H_6	Disilane	8	2169 - 130	18	287-292
CH_3N	Methanimine	5	3262 - 1058	9	293-297	SiH_2	Silylene	3	1995 - 998	3	298
CH_3NO	Formamide	6	3563 - 288	12	299,300	SiH_2Cl_2	Dichlorosilane	5	2237 - 188	9	301
CH_4	Methane	5	3018 - 1310	9	302	SiH_3Cl	Chlorosilane	5	2201 - 550	9	303,304
CH_3O	Methanol	6	3682 - 199	12	305	SiH_3F	Fluorosilane	5	2209 - 729	9	306,307
CH_3S	Methanethiol	6	3010 - 234	12	19,308-312	SiH_4	Silane	5	2189 - 913	9	313-315
CH_3N	Methanamine	7	3424 - 264	15	316-320	SiHCl_3	Trichlorosilane	5	2260 - 175	9	321
CH_3P	Methylphosphine	7	3002 - 219	15	322	SiH_2F_3	Trifluorosilane	5	2315 - 305	9	323-326
CH_3Si	Methylsilane	8	2981 - 187	18	327,328	$^1\text{CH}_2$	Methylene	3	2864 - 1352	3	329-331
CHCl_3	Chloroform	5	3032 - 260	9	332-337	SiO	Oxosilene	2	1241 - 1241	1	338
CHF_3	Fluoroform	5	3018 - 507	9	339-341	SO_2	Sulfur dioxide	3	1362 - 517	3	342,343
Cl_2	Molecular chlorine	2	559 - 559	1	344	SO_3	Sulfur trioxide	4	1391 - 497	6	345,346
Cl_2O	Chloro hypochlorite	3	686 - 300	3	347,348	SOCl_2	Thionyl dichloride	4	1251 - 194	6	349-351
ClCN	Carbononitridic chloride	3	2249 - 381	4	352	<i>trans</i> – $\text{C}_2\text{H}_4\text{Cl}_2$	1,2-dichloroethane	8	3018 - 137	18	353
ClF	Chlorine fluoride	2	773 - 773	1	354	$^3\text{CH}_2$	Methylene	3	3213 - 963	3	355,356
ClF_3	Trifluoro- λ^3 -chlorane	4	751 - 328	6	357						

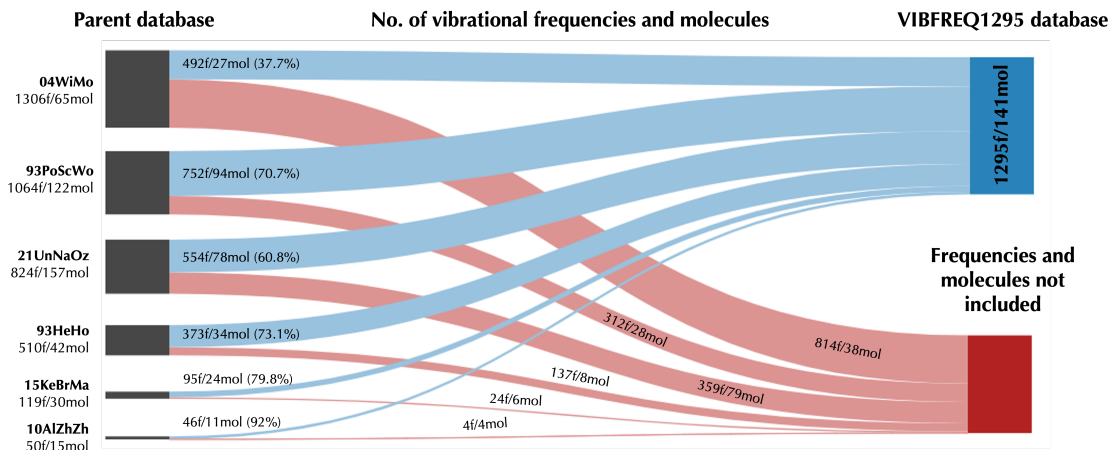


Figure 1: Vibrational frequency databases (left) used in the development of VIBFREQ1295 (upper-right blue panel). These databases correspond to the works of Witek and Morokuma¹⁸ (04WiMo - 1306f/65mol), Pople et al.¹³ (93PoScWo – 1064f/122mol a.k.a. the F1 set), Ünal et al.¹⁹ (21UnNaOz – 824f/157mol), Healy and Holder²⁰ (93HeHo – 510f/42mol), Kesharwani et al.²¹ (15KeBrMa – 119f/30mol), and Alecu et al.²² (10AlZhZh – 50f/14mol). The notation $(x)f/(y)mol$ indicates the total number of frequencies x and molecules y considered in each database. The same notation is used to indicate the number of frequencies and molecules from each database that were included (upper-right blue panel) and were not (lower-right red panel) included into VIBFREQ1295.

describing their original source of data when compiling the experimental fundamental frequencies. We chose these databases based on the heterogeneity of the molecules considered to guarantee minimal overlap of molecules between the different sets. In Figure 1 we present the six databases considered, showcasing the size of each database as indicated by the notation $(x)f/(y)mol$, where x and y represent the total number of frequencies and molecules, respectively. It is worth mentioning some other databases of critically evaluated experimental data, especially the Computational Chemistry Comparison and Benchmark Database (CCCBDB),³⁵⁸ the compilation of experimental vibrational frequencies by Shimanouchi,³⁵⁹ and the database collated by Huber and Herzberg.³⁶⁰ Though these bigger databases contain additional molecules and data that could be used to expand our new database, we chose to align more closely with the heritage of previous database collation for vibrational frequency scaling factors, which were often extracted from these larger databases.

As displayed in Figure 1, not all molecules and frequencies from the former databases were included into VIBFREQ1295. Instead, we curated the initial data by considering only molecules fulfilling three main criteria:

Table 2: Parent databases considered in the development of VIBFREQ1295.

Database	Alias	Reference	Freqs	Mols	Data Origin
04WiMo	1306f/65mol	Witek and Morokuma ¹⁸	1306	65	Largely based on the Computational Chemistry Comparison and Benchmark Database (CCCBDB). ³⁵⁸
93PoScWo	1064f/122mol	Pople et al. ¹³	1064	122	Frequencies collected from the herculean work of Shimanouchi. ³⁵⁹ Widely implemented in the calculation of scaling factors as evidenced by Scott and Radom. ¹²
21UnNaOz	842f/157mol	Ünal et al. ¹⁹	824	157	Largely based on the Computational Chemistry Comparison and Benchmark Database (CCCBDB). ³⁵⁸
93HeHo	510f/42mol	Healy and Holder ²⁰	510	42	Largely based on the Computational Chemistry Comparison and Benchmark Database (CCCBDB). ³⁵⁸
15KeBrMa	119f/30mol	Kesharwani et al. ²¹	119	30	Combination of experimental and computational data taken from the CCCBD set ³⁵⁸ and the Huber and Herzberg compilation, ³⁶⁰ as well as from individual studies.
10AlZhZh	50f/15mol	Alecu et al. ²²	50	15	Based on the NIST Web book ³⁶¹ and the CCCBD set. ³⁵⁸

1. Rigid molecules with only one energetically-relevant low-lying conformer (this was assessed using the CREST³⁶² and CENSO³⁶² packages for conformer sampling with default values);
2. Small- to medium-sized molecules with no more than 14 total atoms and 6 non-hydrogen atoms; and
3. Molecules with easily accessible and reliable gas-phase experimental fundamental frequencies reported in the literature.

The light-blue areas connecting the nodes in Figure 1 schematically represent the number of molecules and frequencies from each database that have been considered into VIBFREQ1295, along with the percentages they represent in their parent database. In most cases, we included > 60 % of the molecules and frequencies from the parent databases, except for the 1306f/65mol (04WiMo)¹⁸ set, where only 37.7 % of the data was considered. The light-red areas in the figure, on the other hand, represent the proportion of data that was excluded from our database. This data mostly consists of a combination of molecules that (1) exceed the 14 total atoms criteria, (2) have incomplete frequency assignments, and (3) rely on experimental fundamental frequencies recorded in liquid-phase or with matrix isolation techniques. Note that despite disregarding this data from the database, VIBFREQ1295 is still large in terms of the number of experimental fundamental

frequencies considered.

To avoid carrying forward potential misassignments in the fundamental frequencies, we performed a thorough literature search to search for potential updates to the original experimental fundamental frequencies for all molecules in our database. Frequencies from newer publications replaced the original data when either (1) the new publication had data at a significantly higher resolution (usually rovibrational resolved vs unresolved) and (2) the new publication explicitly discussed and justified the reassignments of the experimental data (often with computational or extra experimental evidence).

Figure 2 presents a histogram of the compiled experimental data as a function of the year of publication. We observe that, whilst the time-length of publications spans between the 1950s to 2020, 39.3 % of the collated data (i.e., 509 fundamental frequencies) have been published since 2000.

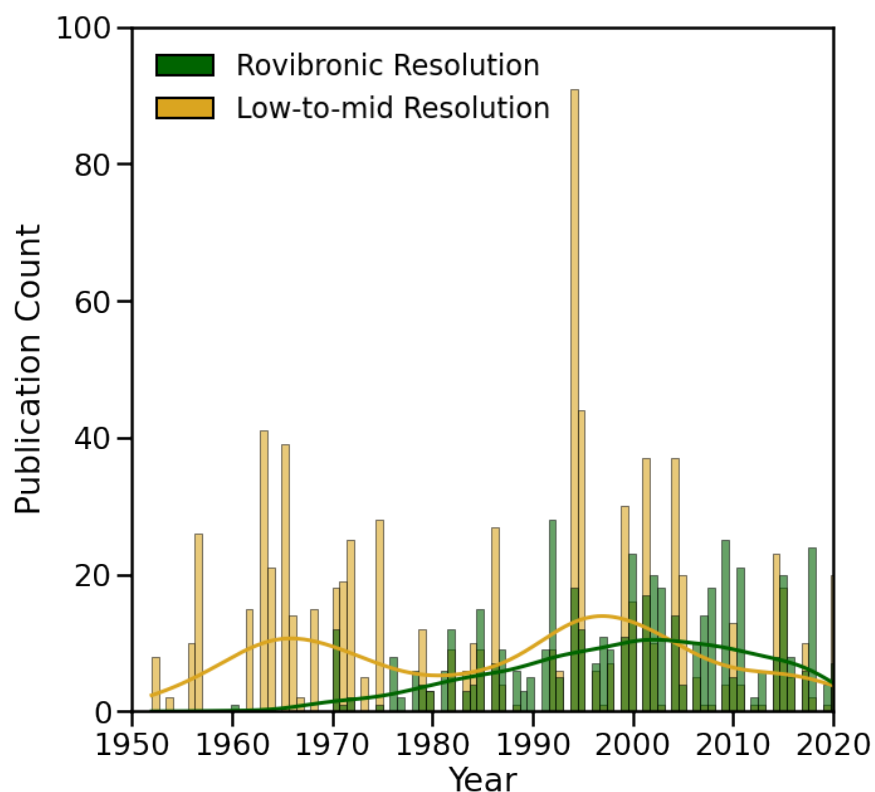


Figure 2: Distribution of the year of publication for the experimental data compiled in the present work. Green and yellow are used to distinguish between publications with rovibronic and low-to-mid resolution, respectively.

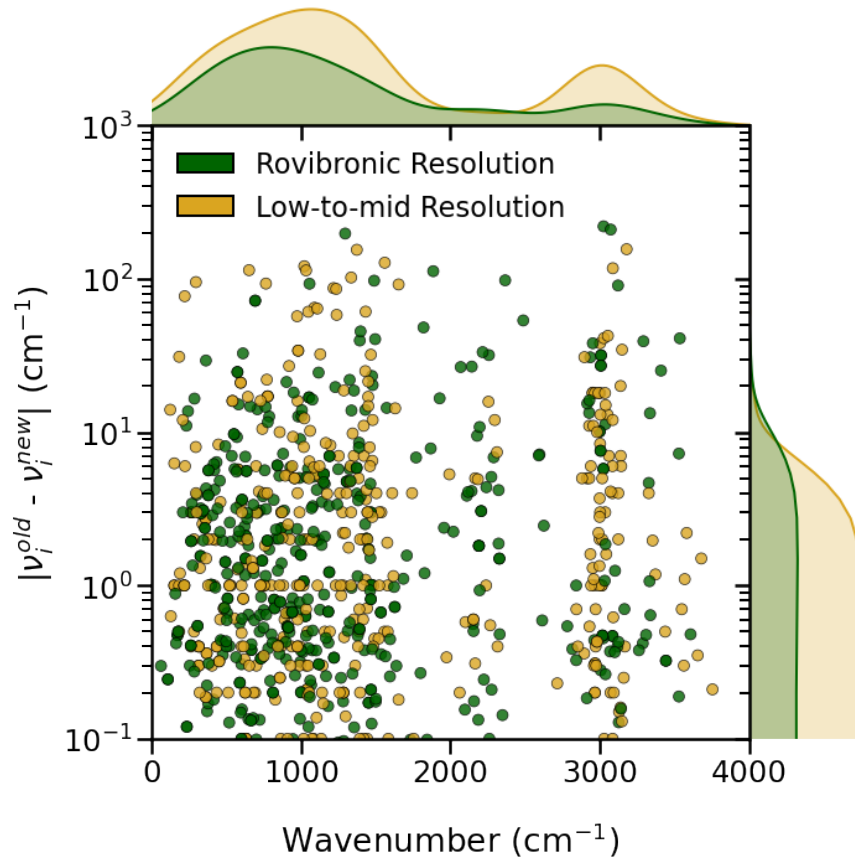


Figure 3: Absolute deviation (in logarithmic scale) between the former (ν_i^{old}) and updated (ν_i^{new}) experimental fundamental frequencies ($|\nu_i^{old} - \nu_i^{new}|$) in VIBFREQ1295. The plots on the top and right-side of the figure illustrate the density distribution of the data across the whole frequency and absolute deviation ranges, respectively. Differences below 10^{-1} cm^{-1} are not displayed in the figure.

Figure 2 also highlights the experimental resolution of the data, a good indication of likely uncertainty in the reported experimental figure. 497 of the collected frequencies (38 %) have rovibronic resolution, whereas the rest of the database consists of fundamental frequencies recorded at low- to mid-resolution.

To understand the importance of the data update, Figure 3 presents the absolute difference (in logarithmic scale) between the frequencies reported in the parent databases (ν_i^{old}), and the frequencies collected from our new literature search (ν_i^{new}), i.e., $|\nu_i^{old} - \nu_i^{new}|$. The plots on the top and right-side of the figure illustrate the density distribution of the data in each axis. Large errors concentrate in the region below 1500 cm^{-1} (the low-frequency region) and around 3000 cm^{-1}

Table 3: Frequency difference, $|v_i^{old} - v_i^{new}|$ (in cm^{-1}), breakdown between the former v_i^{old} and updated v_i^{new} values in VIBFREQ1295.

$ v_i^{old} - v_i^{new} $	Percentage (%)	No. of Frequencies
Identical	30.4	394
(0 – 1]	34.4	445
(1 – 10]	24.7	320
(10 – 50]	8.11	105
> 50	2.39	31

Table 4: Molecules with an absolute frequency difference, i.e., $|v_i^{old} - v_i^{new}|$, larger than 50 cm^{-1} . The potential reason behind these discrepancies is provided in the table, as well as the references to the former and updated frequency assignments.

Molecule	Mode	Former Freq. (cm^{-1})	Former Reference	New Freq. (cm^{-1})	New Reference	$ v_i^{old} - v_i^{new} $ (cm^{-1})	Reason
BH	1	2367.0	Fernando and Bernath ²⁶	2269.2	Fernando and Bernath ²⁶	97.773	Former frequency was harmonic
² BO	1	1885.0	Melen et al. ³⁶	1772.9	Melen et al. ³⁶	112.14	Former frequency was harmonic
C ₂ H ₅ F	8	1048.0	Pople et al. ^{13*}	1109.0	Dinu et al. ¹⁴⁷	61.000	Potential missassignment
	16	1108.0		1172.0		64.000	
C ₂ H ₆ S	14	973.00	Witek and Morokuma ^{18*}	1030.0	Ellwood et al. ¹⁶³	57.000	Potential missassignment
C ₄ N ₂	3	692.00	Chase et al. ³⁶³	620.00	Winther and Schönhoff ²⁴⁰	72.000	Potential missassignment
CH ₂ S	5	3180.7	Yachmenev et al. ³⁶⁴	3024.6	Johns and Olson ²⁷⁶	156.07	Former frequency was harmonic
	1	3088.2		2971.0		117.21	
CH ₄ O	12	250.00	Healy and Holder ^{20*}	199.80	Twagirayezu et al. ³⁰⁵	50.200	Potential missassignment
CH ₃ P	5	1238.0	Ünal et al. ^{19*}	1296.2	Kim and Zeroka ³²²	58.200	Potential missassignment
CSCl ₂	3	220.00	Pople et al. ^{13*}	297.00	Frenzel et al. ⁷⁶	77.000	Potential missassignment
² HCO	1	2488.0	Pople et al. ^{13*}	2434.5	Dane et al. ¹²³	53.522	Potential missassignment
HO ₂	2	1489.0	Ünal et al. ^{19*}	1391.8	Burkholder et al. ¹⁵⁰	97.246	Potential missassignment
	3	1295.0		1097.6	Nelson and Zahniser ¹⁴⁹	197.38	
c-C ₃ H ₃ NO_1	13	764.00	Witek and Morokuma ^{18*}	857.10	Robertson ⁴⁴	93.100	Potential missassignment
	12	1021.0		900.20		120.80	
	16	651.00		764.90		113.90	
	4	1653.0		1561.1		91.900	
	5	1560.0		1432.6		127.40	
	6	1432.0		1370.9		61.100	
	7	1373.0		1218.3		154.70	
	8	1217.0		1130.0		87.000	
	10	1089.0		1024.20		64.800	
	11	1033.0		919.50		113.50	
c-C ₄ H ₄ N ₂	3	1335.0	Witek and Morokuma ^{18*}	1233.0	Hewett et al. ⁵⁹	102.00	Potential missassignment
	17	1235.0		1149		86.000	
¹ CH ₂	1	3026.0	Pople et al. ^{13*}	2806.1	Petek et al. ³³⁰	219.93	Potential missassignment
	3	3074.0		2864.5	Petek et al. ³²⁹	209.50	
³ CH ₂	2	1056.0	Pople et al. ^{13*}	963.10	Marshall and McKellar ³⁵⁵	92.901	Potential missassignment
	3	3123.0		3213.5	Jensen and Bunker ³⁵⁶	90.500	

(*) Note that the compilation paper, i.e., the parent vibrational frequency database, is referenced when the original experimental publication was not available.

where the C–H stretching frequencies dominate; however, these are also the regions where more data is available.

Interestingly, the resolution at which the fundamental frequencies have been recorded does not significantly influence the similarity between the former and updated frequencies.

Table 3 presents the frequency difference breakdown between the former and updated values. Note that the first row in the table corresponds to frequencies where no updated experimental values were found in the literature (this data is not displayed in Figure 3). The last row in the table, on the other hand, shows the number of frequencies for which the difference between the former and updated values differs by more than 50 cm^{-1} . We can attribute two main factors to the large discrepancies in these cases: (1) former data corresponding to experimentally-derived harmonic frequencies rather than fundamental frequencies (VIBFREQ1295 consists of experimental fundamental frequencies only), and (2) potentially unnoticed missassignments in the parent databases. In Table 4 we present the former and updated frequencies for these molecules, along with the absolute frequency difference $|v_i^{old} - v_i^{new}|$, and the references to the original and updated experimental publications.

Database Overview

Chemical Space and Molecular Classes

Understanding the chemical nature underpinning the database is essential for delimiting the scope of its applications. In this section, we will compare the chemical composition of the molecules in VIBFREQ1295 with those from four benchmark databases in computational quantum chemistry: the popular general-chemistry sets MGCDB84³⁶⁵ and GMTKN55,³⁶⁶ both containing reference values for thermochemistry, isomerisation energies and kinetics; as well as the specialised Dip152³⁶⁷ and Pol132³⁶⁸ databases, storing benchmark dipole moments and static polarisabilities for small molecules, respectively. For the sake of completeness, we also make comparisons against the popular 1064f/122mol vibrational frequencies database collated by Pople *et al.*¹³

Figure 4 displays the range of elements available in VIBFREQ1295, along with the percentage of molecules containing each element individually. We can observe that the element composition in the database is constrained to molecules containing nonmetal and halogen atoms, with a small percentage of molecules containing the less common B, Si and Al elements. Thus, future applications of VIBFREQ1295 should focus towards general-chemistry properties of rigid organic-like molecules only.

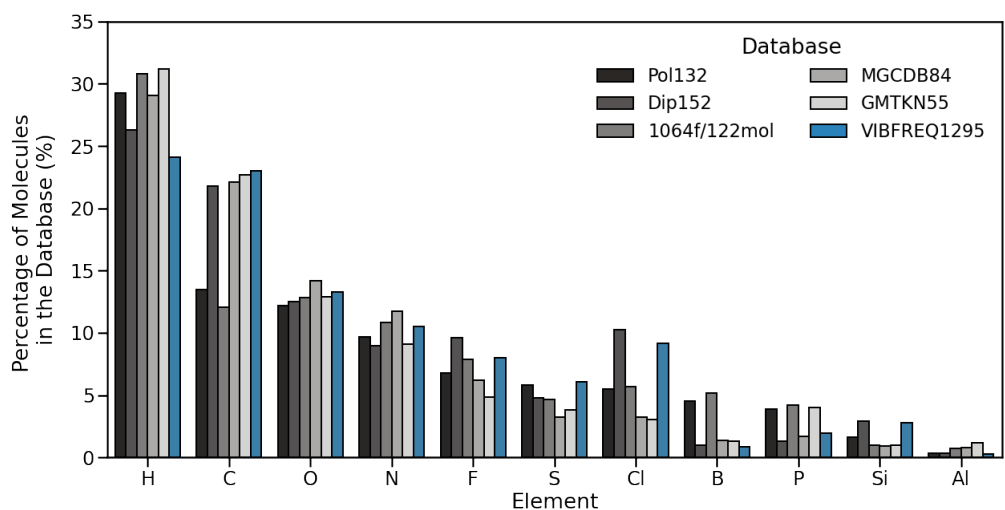


Figure 4: Comparison of the distribution of elements (in percentage of molecules) across the six benchmark databases considered: in blue, VIBFREQ1295, introduced in the present paper; and in shades of grey Pol132,³⁶⁸ Dip152,³⁶⁷ 1064f/122mol,¹³ MGCDB84,³⁶⁵ and GMTKN55,³⁶⁶ respectively. Note that, apart from VIBFREQ1295, the other databases may also have molecules containing elements different than those displayed in the figure.

Figure 4 also compares the molecular element compositions of VIBFREQ1295 with those from the other general-chemistry and specialised databases. Note that the percentages in the figure are indicative only, as the naming convention for some molecules in the databases was not consistent. All six databases share a similar trend in element composition focusing particularly in organic-like molecules containing H, C, O, N and halogens (except for the Pol132 and 1064f/122mol sets where C-containing molecules are less prominent). Even though 70.7 % of the data from 1064f/122mol was included into VIBFREQ1295 (see Figure 1), the figure shows some significant differences in the percentages for both sets, especially for Cl-containing molecules where VIBFREQ1295 is particularly large. We can attribute this difference to the widespread of Cl-containing molecules in

the other vibrational frequency databases considered.

To allow further comparisons, we categorised the list of all molecules in the six databases into three main classes:

1. **CHNOPS Molecules:** molecules containing C, H, N, O, P and S only (e.g., $\text{c-C}_4\text{H}_4\text{O}$, C_2N_2);
2. **Halogens:** any molecule containing a halogen element (e.g., AlCl_3 , SiH_3F); and
3. **Others:** molecules containing any other element from the periodic table, except for halogens (e.g., BH_3CO , CH_6Si); and

The pie charts in Figure 5 show the percentages for each molecular class in the different databases considered. *CHNOPS-like* molecules dominate across all databases, especially in the VIBFREQ1295, GMTKN55 and MGCDB84 sets with more than 50 % of the molecules falling within this class. Molecules belonging to the *Others* class are scarce in VIBFREQ1295 (only 5.7 % of the database), mostly due to the absence of species containing B, Si and Al (see Figure 4), similarly to the 1064f/122mol and MGCDB84 sets which also seem to underestimate this molecular class. Nonetheless, VIBFREQ1295 is notably rich in halogenated compounds (almost 40 % of the database), which correlates with the large percentage of Cl-containing molecules in the database. As both *CHNOPS-like* and halogenated compounds share similar percentages in VIBFREQ1295, we do not expect significant biases towards a particular class in future applications (see Section). However, we caution the user about the potential overestimation of halogenated compounds in VIBFREQ1295.

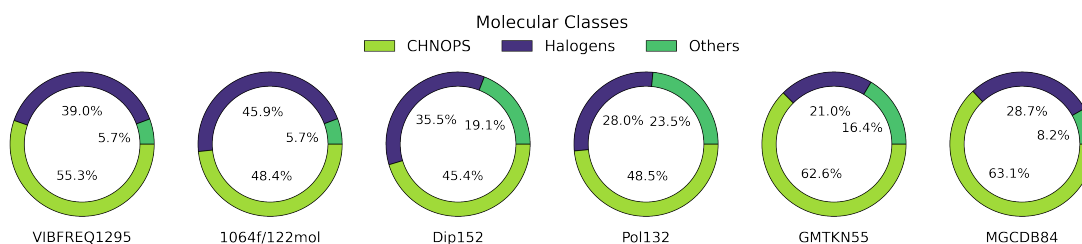


Figure 5: Proportion of molecules in the databases considered that fall within the three molecular classes defined in present work: CHNOPS, Halogens, and Others.

Functional Groups

We wrote a python code based on the RDKit library³⁶⁹ to obtain the counts of the different functional groups in our database. A comprehensive description of all functional groups can be found in Table S1 in the supplemental material for this paper.

Figure 6 illustrates some of the functional groups present in VIBFREQ1295, along with their indicative counts in parenthesis. In line with the predominance of F- and Cl-containing species, halogen-containing functional groups dominate in the database, particularly due to the ubiquitous presence of the E-X group (where *E* represents any element apart from C, and *X* is a halogen), having the largest count across all functional groups. Hydrocarbon groups are also widespread in the database, with a large proportion of molecules containing alkane- and alkene-like groups. Note that the variety of O-containing groups is extensive, with multiple functional groups containing pairs of heteroatoms including O, e.g., R-NO₃ (nitrate) or R₁-SO-R₂ (sulfoxide).

Vibrational Modes

Functional groups are not only responsible for driving chemical reactivity, but also help distinguishing between molecules based on their vibrational motions. As functional groups correspond to well-defined regions of the molecule containing specific atoms (e.g., C=O group), it is straightforward to identify the localised vibrations of those functional groups in the infrared spectrum (e.g., C=O stretch at $\sim 1700\text{ cm}^{-1}$).

In VIBFREQ1295, we provide approximate descriptions for all vibrational modes in the database, based on the vibrational motions from our quantum-chemistry calculations (see Section). Note that these descriptions are indicative only; Highly-coupled modes and descriptions in the low-frequency range (usually below $1,000\text{ cm}^{-1}$) are less accurate due to the large number of atoms and bonds involved in the vibration.

Figure 7 presents the density distribution for the 20 most common vibrational modes in the database. The numbers in parenthesis indicate the counts for each vibrational mode, with central frequencies displayed in the right-most side of the figure. We can observe that the database has

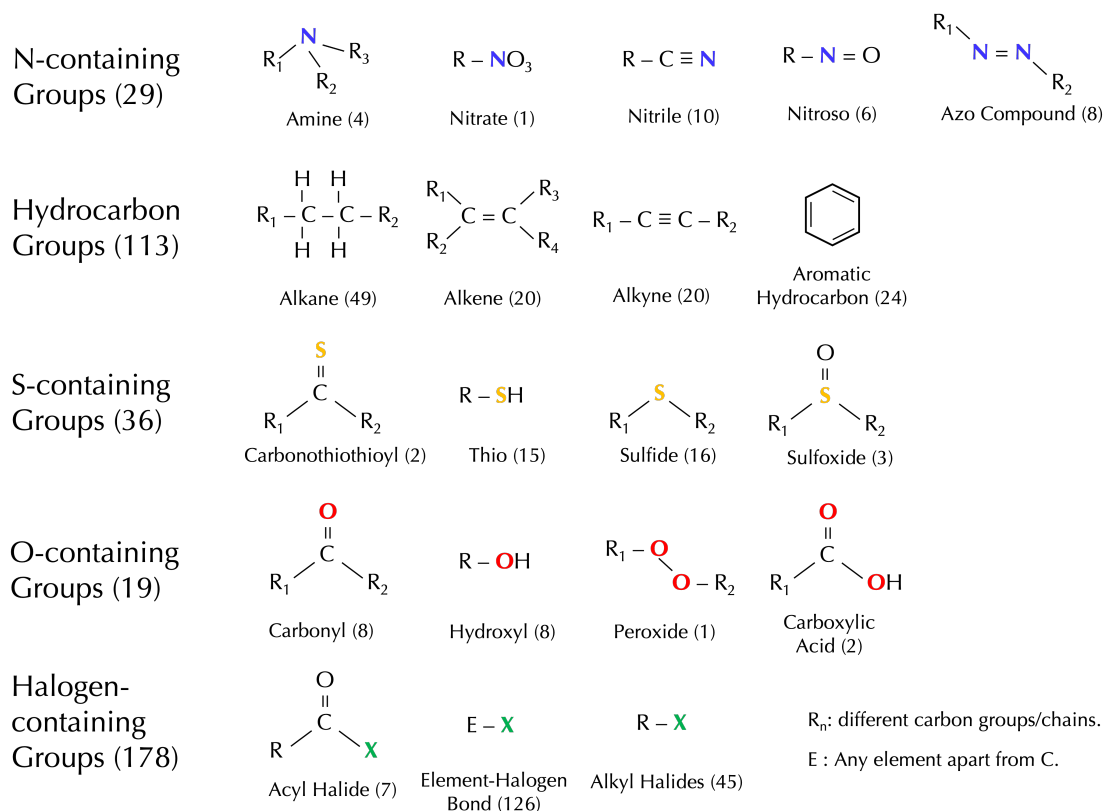


Figure 6: Schematic representation of popular functional groups in organic chemistry present in VIBFREQ1295. The functional groups are sorted based on their element composition. The numbers in parenthesis are indicative of the occurrence of the functional groups in the database. R_n is used to denote C-containing groups or chains, and E represents any element from the periodic table apart from C.

a good coverage in terms of vibrational modes, spanning between the far- ($10 - 400\text{ cm}^{-1}$) and mid-infrared ($400 - 4,000\text{ cm}^{-1}$) regions. Popular modes like the C-H and O-H stretches are well-defined in the database, with their expected central frequencies lying at approximately $3,000$ and $3,600\text{ cm}^{-1}$, respectively. However, non-stretch modes were more difficult to define uniquely and we kept the terms fairly generic - e.g., C-H angle and CH_2 bend are used as classifiers for a variety of different vibrational motions (including some wagging, rocking, twisting and scissoring modes) and thus they span a wider frequency range. The figure also shows that, as expected, vibrational modes involving more than two atoms, or relatively heavy elements, e.g., S, Cl, lie in the low-frequency range of the spectrum (usually below $1,000\text{ cm}^{-1}$).

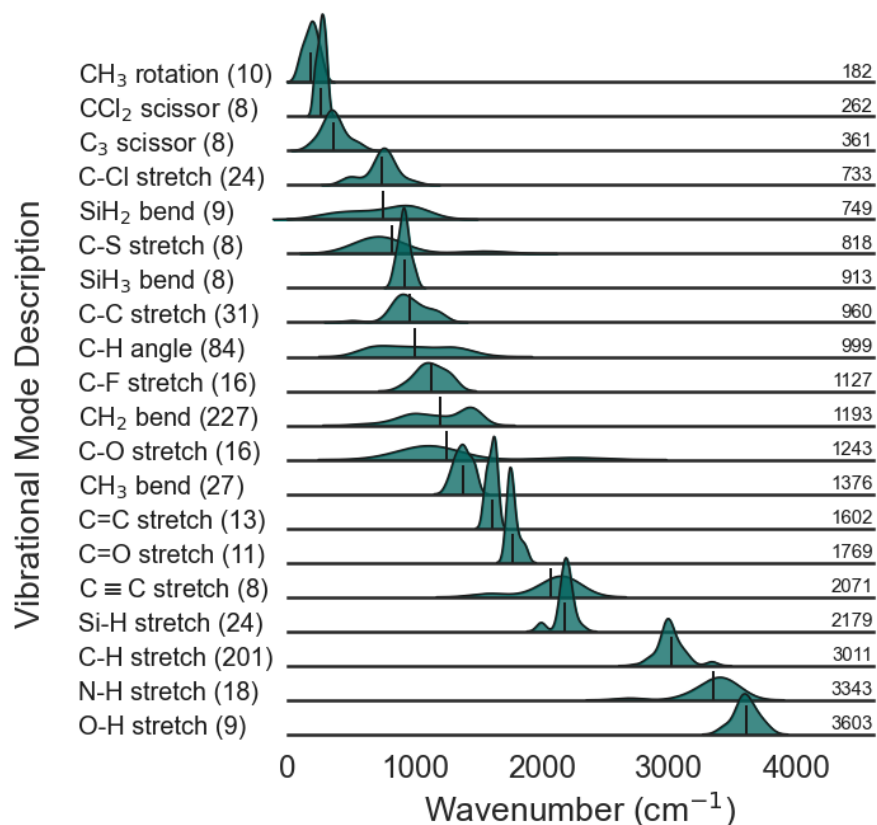


Figure 7: Density distribution of the 20 most popular vibrational modes in VIBFREQ1295. The numbers in parenthesis correspond to the number of entries of each vibrational mode in the database. The central frequencies for the functional group are displayed in the right-most side in the figure, as well as visually represented as vertical lines in the corresponding density distribution.

Applications for this database

It is clear that the primary use of VIBFREQ1295 is to allow benchmarking of the performance of model chemistries for harmonic frequency calculations. We are currently undertaking a benchmarking study quantifying the quality of scaled harmonic vibrational frequencies produced from a wide cross-section of density functional approximations, and double and triple-zeta basis sets. Future studies considering the performance of various anharmonic treatments, e.g., VPT2 and VSCF, are natural and important follow-ups.

It is possible that future density functional theories or basis sets could utilise this vibrational frequency data as part of their training data, perhaps producing approximations specifically tuned to this property. However, this is less likely than for other experimental property databases because (1) frequencies are computationally expensive calculations, and (2) vibrational frequencies are not a particularly challenging property for model chemistries to predict as anharmonicity error dominates over model chemistry error very quickly.¹¹

Instead, more promising applications could be directed towards machine learning algorithms. Models trained on the VIBFREQ1295 experimental data could predict fundamental frequencies of small molecules either entirely without computational quantum chemistry, or as corrections to these calculations. For instance, The RASCALL computational chemistry approach⁹ uses experimental fundamental frequencies (mostly from common organic functional groups) to predict approximate spectral data for thousands of molecules simultaneously. RASCALL could benefit from the distribution of vibrational frequencies collated here for multiple functional groups, as this data can help considering the effects of the chemical environment in the vibrational frequency for a given functional group, i.e., how the frequency for the functional group vibration shifts according to the atoms and chemical groups surrounding it (see Figure 7).

Another potential application of VIBFREQ1295 is providing a centralised repository of high-level *ab initio* harmonic frequencies for supporting approaches seeking more accurate vibrational spectra predictions. This is the case of, for example, the hybrid approach implemented by Biczysko *et al.*³⁷⁰ where CCSD(T)-like harmonic frequencies for a given molecule are corrected by means

of anharmonic calculations (usually VPT2) performed at a computationally less-demanding model chemistry choice, e.g., hybrid functionals and double-zeta basis sets. This hybrid approach has proved to deliver satisfactory performance in small-to-medium-sized molecules.^{371–373}

It is not only the experimental and theoretical harmonic frequencies in VIBFREQ1295 that can be practical; the set of compiled literature references for each molecule are a useful starting point for more detailed spectral data compilation such as model Hamiltonians fits or assigned rovibrational transitions. These higher-resolution data are crucial for enabling remote molecular identification and environmental characterisation in complex gaseous environments including planetary atmospheres.^{374–376}

High-quality *ab initio* Harmonic Frequencies: Comparison with Experiment

Computational Details

To complement the experimental fundamental frequencies collated here, we also calculated high-level *ab initio* harmonic vibrational frequencies for all 141 molecules. Initial molecular geometries were obtained from their SMILES identifiers through an automated approach using the RDKit³⁶⁹ and ChemCoord³⁷⁷ libraries in python.

We performed all harmonic frequency calculations using the CCSD(T)(F12*) method¹⁵ together with the cc-pVDZ-F12 basis set.^{16,17} We chose this model chemistry based on recommendations by Martin and Kesharwani³⁷⁸ and Schmitz and Christiansen,³⁷⁹ who found a fast basis set convergence at a reasonable computational cost for this model chemistry. Indeed, they reported errors between 3–4 cm⁻¹ in the computed harmonic frequencies when compared against CCSD(T) limit results.

The initial geometries for the calculations were optimised using a tight convergence criteria, with maximum force and maximum displacements smaller than 1.5x10⁻⁵ Hartree/Bohr and

6.0×10^{-5} Å, respectively. Default values were used for the CABS singles (1.0×10^{-8}) and CCSD convergence (1.0×10^{-6}) thresholds. A template of the input file used in the calculations is provided in the supplemental material for this paper. All calculations were carried out using the MOLPRO 2020 quantum chemistry package.³⁸⁰

Calculating Scaling Factors: The Test and Training Set Separation

Scaling factors are essential for comparing calculated harmonic frequencies with experimental fundamental frequencies.¹¹ The standard approach usually involves fitting and testing the scaling factor using the same set of fundamental frequencies without distinguishing between independent training and test sets.

Here, however, in line with good-practice procedures in data science, we computed our scaling factor by splitting the database into two different sets: a training set, used in the fitting of the scaling factor, and a test set to evaluate the performance of the computed scaling factor. Both the training and test sets have been assigned with similar percentage compositions in terms of the molecular classes (halogens $\sim 29\%$ and non-halogens $\sim 71\%$), and vibrational modes (stretch $\sim 44\%$ and non-stretch $\sim 56\%$) considered. Ensuring high similarity between the training and test sets is pivotal for extrapolating conclusions.

To analyse how sensitive the scaling factor and scaling factor’s performance are to the partition of the database, we split VIBFREQ1295 into four different groups of training and test sets: 100 – 0, 90 – 10, 80 – 20, and 70 – 30, where the numbers in each pair correspond to the percentages of data from VIBFREQ1295 included in the training and test sets, respectively. The first partition group (100 – 0) corresponds to the standard approach of using the whole set of data to fit and test the scaling factor.

In all cases, we used the training set to calculate the corresponding scaling factor λ as $\lambda = (\sum_i^N \omega_i v_i) / (\sum_i^N \omega_i^2)$, where ω_i and v_i represent the calculated harmonic and experimental fundamental frequencies, respectively, and both summations run over the total number of frequencies N considered in the training set. The calculated scaling factors were then used to scale the raw

harmonic frequencies in the corresponding test sets, with performance judged by the root-mean-squared-error (RMSE), the standard statistical metric for assessing performance,¹¹ between the scaled harmonic and experimental fundamental frequencies as $\text{RMSE} = \sqrt{(\sum_i^N (\lambda \omega_i - \nu_i)^2) / N}$.

To ensure convergence in the reported metrics, we randomised the partition of the training and test sets over 100 cycles, calculating each time the scaling factor and corresponding RMSE. We present the average results with their standard deviations in Table 5 for both the training and test sets, separately, across the different partition groups.

Table 5: Training and test sets groups used in the calculation of scaling factors for the CCSD(T)(F12*)/cc-pVDZ-F12 harmonic frequencies. Numbers in parenthesis are one standard deviation in the last digit of the reported value, calculated from 100 different training/test partitions of full dataset.

Scaling Factor	%	Training Set	%	Test Set
		RMSE (cm ⁻¹)		RMSE (cm ⁻¹)
0.9617	100	33	0	-
0.9618(2)	90	33 (1)	10	31 (6)
0.9618(3)	80	33 (1)	20	32 (5)
0.9617(3)	70	33 (2)	30	32 (4)

Table 5 shows that virtually the same metrics are obtained for both the training and test sets across the different partition groups, ensuring high similarity between both sets, and thus negligible overfitting in the computed scaling factors. This implies that the metrics obtained from our analysis represent a fair indication of our model chemistry and scaling factor performance. Looking at the different partition groups in Table 5, there is no major differences in the statistical figures reported; however, the overall small standard deviation in the test set for the 70 – 30 split highlight as a good compromise for future calculations. Therefore, further discussions in this paper will focused on calculations using the 70 – 30 split (with metrics hereafter referred as the global scaling factor), unless otherwise noted.

It is worth noting that the global scaling factor optimised here for the CCSD(T)(F12*)/cc-pVDZ-F12 model chemistry (0.9617(3)) is essentially identical to the scaling factor of 0.9627 found by Kesharwani *et al.*²¹ for the CCSD(T)(F12*)/cc-pVQZ-F12 model chemistry. This fur-

ther validates our previous finding suggesting convergence of the scaling factor at quite moderate computational levels,¹¹ e.g., hybrid functional with double-zeta basis sets, thus suggesting the potential implementation of universal scaling factors for model chemistries above the hybrid/double-zeta level.

Robust Error Quantification: Comparing Theory with Experiment

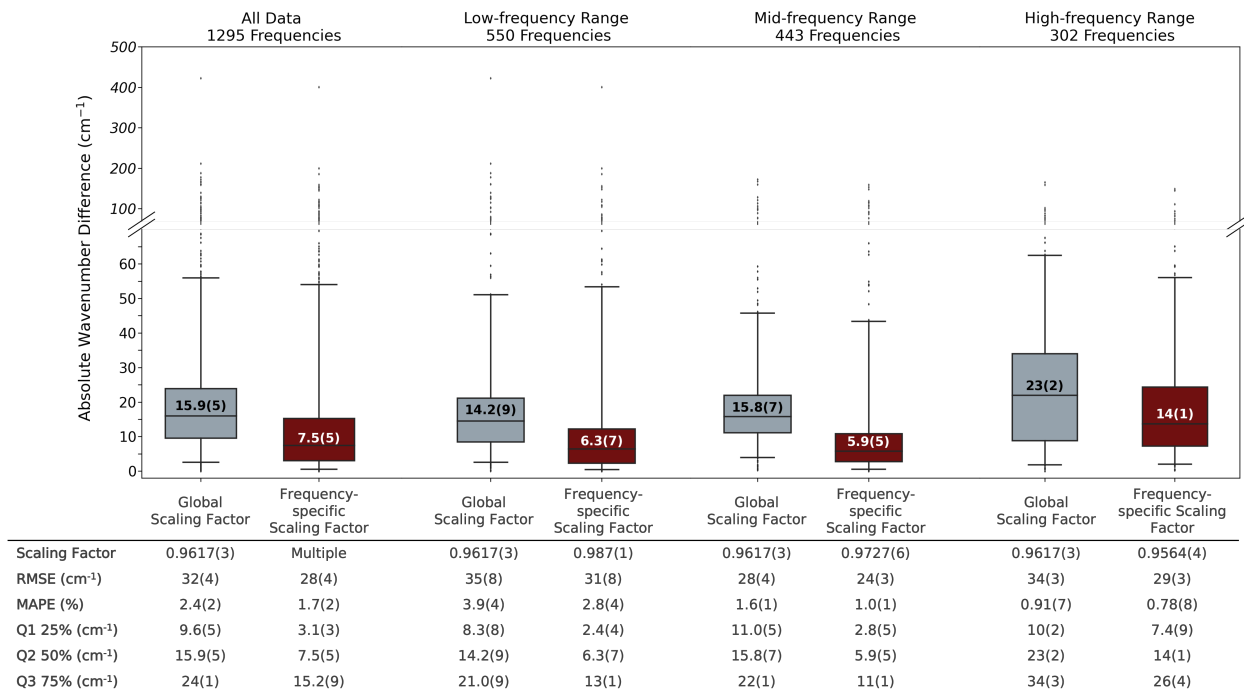


Figure 8: Absolute wavenumber difference (cm⁻¹) between scaled harmonic and experimental fundamental frequencies using global (grey), and frequency-range-specific (maroon) scaling factors. The numbers inside the boxes represent the median values for each classification. A scale discontinuity in the y-axis (at approximately 70 cm⁻¹) has been imposed to highlight both the box and whiskers, and the outliers in the data. The table at the bottom presents the scaling factor, RMSE, Mean Absolute Percentage Error (MAPE), as well as the first, second (median), and third quartiles for the data distribution in each classification individually. The bottom and top whiskers in the figure encapsulate 5 % and 95 % of the data, respectively. Numbers in parenthesis are one standard deviation in the last digit of the reported values as calculated over 100 cycles of the 70%/30% training/test partitioning of the dataset.

The conventional approach for quantifying error in harmonic frequency calculations requires comparing experimental fundamental frequencies against calculated harmonic frequencies that have been scaled using a global scaling factor (e.g., 0.9617(3) in Table 5). However, as noted

by the early work of Scott and Radom,¹² this procedure fails in properly describing low-frequency vibrations as it inherently gives more weight to frequencies lying at the upper end of the vibrational spectrum. Instead, alternative approaches have opted for calculating scaling factors for different frequency regions leading to differences in performance.^{381–389}

The standard cutoff for distinguishing between low- and high-frequency vibrations is usually set at $1,000\text{ cm}^{-1}$.³⁸² However, based on a detailed analysis examining the effect of multiple frequency thresholds (further explained in the supplemental material), we defined three different regions of importance: low-frequency ($< 1,000\text{ cm}^{-1}$), mid-frequency ($1,000 - 2,000\text{ cm}^{-1}$), and high-frequency ($\geq 2,000\text{ cm}^{-1}$) vibrations.

In Figure 8 we present the absolute wavenumber difference (in cm^{-1}) between the scaled harmonic and experimental fundamental frequencies for the defined frequency regions using the following scaling factors: in grey, using the global scaling factor (0.9617(3)) reported in Table 5; and in maroon, using scaling factors optimised for the low- (0.987(1)), mid- (0.9727(6)), and high-frequency (0.9564(4)) regions. Note that the frequency-range-specific scaling factors were calculated by only considering frequencies falling within each range, e.g., the scaling factor for the low-frequency region was calculated by considering frequencies below $1,000\text{ cm}^{-1}$ only. The number of frequencies in each frequency region is displayed at the top of the figure. The left-most boxes compare the performance of using the global and frequency-range-specific scaling factors in the whole set of data, whereas the rest of the figure compares performance for each frequency range individually. The corresponding scaling factors, RMSEs, mean absolute percentage errors (MAPE), as well as we the first, second (also displayed inside each box), and third quartiles are presented in the table at the bottom of the figure.

Overall, the figure shows a significant improvement in the absolute wavenumber difference when introducing frequency-range-specific scaling factors in the calculations (medians of $15.9(5)$ vs $7.5(5)\text{ cm}^{-1}$ for the global and frequency-range-specific scaling, respectively). This result suggests that the error in the scaled harmonic frequencies is not constant, but changes gradually with the frequency region and, thus, justifies the implementation of frequency-range-specific over global

scaling factors to achieve superior performance. We can confirm this variation by looking at the spread of the absolute wavenumber differences for all three designated frequency regions, where it is evident that the errors generally increase from low- to high-frequency vibrations.

The relatively high errors in the high-frequency range (when using both the global and frequency-range-specific scaling factors) can be explained by inspecting the composition of our database. A closer look into Figure 7 shows that the high-frequency vibrations ($\geq 2,000\text{ cm}^{-1}$) in VIBFREQ1295 are mostly dominated by stretching-like modes, e.g., C–H, O–H, and N–H stretches, which are inherently more anharmonic than other vibrational modes in the database. This is because stretching modes can naturally lead to bond dissociation, a process not contemplated under the harmonic approximation and thus better represented by anharmonic approaches, while most non-stretching modes are harmonically bound. We can further justify this finding by noting the differences in scaling factors between the three designated frequency regions, where the scaling factor decreases from the low- (0.987(1)) and mid- (0.9727(6)), to the high-frequency (0.9564(4)) range (which also supports splitting the vibrational spectrum in three instead of two frequency regions).

Another potential aspect to examine from this compilation of data is whether the reported metrics in Figure 8 are affected by the type of molecules (halogens and non-halogens), or vibrational modes (stretches and non-stretches) in the database. We opted for excluding this analysis from the main manuscript to avoid over-complicating the narrative; however, we encourage the interested reader to look into the detailed description in the supplemental material. Instead, we summarise our findings into three main points:

1. developing scaling factors specifically tuned for halogen and non-halogen molecules is unnecessary as akin performance in the scaled harmonic frequencies is achieved when utilising the global scaling factor (0.9617(3));
2. despite the large counts of halogen-containing molecules in VIBFREQ1295 (see Figure 4 and Figure 5), applications of this database are not likely to be biased towards a particular molecular group as similar scaling factors and statistical metrics were found for halogen-containing and non-halogen-containing molecules; and

3. using mode-specific scaling factors results in an overall improvement in the scaled harmonic frequencies over using a global scaling factor, potentially suggesting the implementation of different scaling factors whenever a particular vibrational mode is considered, as suggested in previous approaches.^{11,390–397} Nonetheless, stretching and non-stretching modes can be generally assigned to the high and low/mid-frequency ranges of the vibrational spectrum, respectively (see Figure 7), implying that both mode-specific and frequency-range-specific scaling factors are accounting for the same corrections and could be potentially interchanged.

In light of these findings and noting that sorting vibrational frequencies based on their frequency position is more straightforward and reliable than assigning vibrational modes from quantum-chemistry calculations (especially for highly-coupled modes), we encourage the use of frequency-range-specific (low-, mid-, and high-frequency ranges) scaling factors to achieve superior performance in harmonic frequencies calculations.

Despite the overall satisfactory performance of introducing frequency-range-specific scaling factors in harmonic frequency calculations, we also found some scaled harmonic frequencies with significant deviations from the experimental values (data points above the whiskers in Figure 8). The reason behind these large discrepancies is unclear to us as no evident trend is observed in terms of the vibrational mode type, frequency range, or molecular geometry for these frequencies. It might be the case that these frequencies correspond to highly couple modes involving different vibrations simultaneously, which could reach the limits of accuracy within the harmonic approximation; unfortunately, however, there is not a straightforward approach to anticipate this behaviour given a random molecule.

We find open-shell molecules have generally larger errors than closed shell molecules, e.g. of the 10 open-shell species, 7 have at least one frequency with calculation error greater than 50 cm^{-1} . This result is in alignment with previous studies that have shown open-shell systems to be challenging for routine computational quantum chemistry calculations.^{398–402} However, it is unclear whether the larger errors in these systems arise purely from increased errors in the computational chemistry method (e.g. from increased multi-reference character in these molecules) or from an

increased error in the harmonic approximation for open-shell systems.

As the frequencies with large deviations only account for approximately 5 % of the data distribution (top whiskers lie at 95 %), we expect their occurrence to be minimal in routine calculations. Table S4 in the supplemental material lists all molecules and frequencies with deviations larger than $\pm 50 \text{ cm}^{-1}$ from experiment, in addition to their corresponding molecular class and vibrational mode description.

The Anharmonicity Error

Assuming that harmonic frequency calculations at the CCSD(T)(F12*)¹⁵/cc-pVDZ-F12^{16,17} level reduce model chemistry error to a minimum, we can quantify the intrinsic error in the harmonic approximation, a.k.a. the anharmonicity error, by comparing the scaled harmonic and experimental fundamental frequencies in the database.

Using the RMSE as a metric of performance, Kesharwani *et al.*²¹ first estimated this error by scaling experimentally-derived harmonic frequencies against experimental fundamental frequencies for a dataset containing 119 frequencies from 30 molecules (see Figure 1). They found that an optimal scaling factor of 0.9627 results in an RMSE of 24.9 cm^{-1} . We found a very similar scaling factor with the data in our database (0.9617(3) in Table 5). However, our computed RMSE ($32(4) \text{ cm}^{-1}$) when implementing the global scaling approach is significantly higher than the Kesharwani *et al.*²¹ value. One potential reason for this deviation lies in the heterogeneity of both data sets, but the approximate errors in our model chemistry choice, e.g., remaining basis set incompleteness error and the lack of higher order correlation effects, could also influence on the accuracy of our results.^{378,379,403}

Using the RMSE as an estimate for anharmonicity error comes with two main limitations: (1) RMSEs are highly influenced by the presence of outliers in the data, and (2) the RMSEs are a single number that doesn't provide information about the distribution of errors. These limitations are evident in the results in Figure 8 where similar RMSEs are obtained for the different frequency regions when using the global or frequency-range-specific scaling factors despite the error distri-

bution clearly improving substantially when using the frequency-range-specific scaling factors.

Instead of the RMSE, the median error (Q2 50 %) for each absolute wavenumber difference distribution visually represents a more appropriate metric for anticipating the error between the predicted scaled harmonic and experimental fundamental frequency. Thus we recommend that median errors be used instead of RMSE when quantifying anharmonicity error because medians are simple to relate to the usual error of a calculation rather than emphasising outliers like RMSEs.

The median anharmonicity error, and its distribution computed here, sets a lower bound to the reliable performance of a faster more approximate model chemistry such as a hybrid or double-hybrid functional with a double or triple-zeta basis set. Though cancellation of errors could reduce the computed anharmonicity error, there is no physical rationale for this and thus lower errors could be unreliable.

Concluding Remarks

Routine quantum-chemistry calculations, e.g., harmonic and anharmonic frequency calculations, have the potential to enable high-throughput approaches for producing approximate spectral data for thousands of molecules of astrochemistry interest.¹⁰ However, it is currently unclear what model chemistry should be used and what errors in frequency predictions should be expected; this is essential information to help assess the usefulness of these high-throughput calculations to astrochemistry.

In order to rigorously assess the errors and quantify the minimum error obtainable by scaling harmonic computed vibrational frequencies (without unreliable cancellation of errors), here we introduce a new benchmark database (VIBFREQ1295) for harmonic frequency calculations containing 1,295 experimental fundamental frequencies, and CCSD(T)(F12*)¹⁵/cc-pVDZ-F12^{16,17} *ab initio* harmonic frequencies for 141 molecules. The database can be found as part of the supplemental material for this publication, as well as through the Harvard DataVerse¹⁴ (<https://doi.org/10.7910/DVN/VLVNU7>).

VIBFREQ1295’s experimental component is a robust and comprehensive compilation of contemporary experimental fundamental frequencies, providing general updates in previous molecular frequency assignments. The set of compiled literature references in the database spans across nearly 80 years of research in spectroscopy, with a significant proportion of the compiled experimental data corresponding to publications between the 1990s and 2020. More than 30 % of the collated frequencies have been recorded at rovibronic resolution, with the rest of the database compiling fundamental frequencies recorded at moderate resolution. This overall update in the vibrational frequencies was crucial in identifying potentially unnoticed misassignments, frequencies recorded in liquid-phase or with matrix isolation techniques, as well as the use of harmonic rather than fundamental frequencies reported in previous benchmark databases.

The primary application of the VIBFREQ1295 experimental data is to assess the performance of computational chemistry methodologies, most importantly determining the best density functional approximations (DFAs) and basis set combinations for routine calculation of vibrational frequencies, improving on the results compiled in Zapata Trujillo and McKemmish¹¹ –this work is currently underway. VIBFREQ1295 can also be used to train machine-learning models for predicting vibrational spectra of organic-like molecules. Further, the references for the high-resolution experimental publications in the database represent a good initial source for more detailed spectral data compilations, e.g., model Hamiltonian fits.

The compiled experimental data is complemented by new CCSD(T)(F12*)¹⁵/cc-pVDZ-F12^{16,17} *ab initio* harmonic frequencies calculations for all molecules. The comparison of the experimental and computed data allowed an in-depth analysis of the anharmonicity error, i.e., the error between the experimental fundamental frequency and scaled harmonic frequencies. The anharmonicity error was previously estimated as 24.9 cm⁻¹²¹ based on RMSE differences between experimental fundamental and scaled harmonic frequencies; however, our analysis shows that median errors are more appropriate than RMSEs in predicting performance given that RMSEs are dominated by outliers rather than typical expected results. With three frequency-range-specific scaling factors (0.987(1) for frequencies < 1000 cm⁻¹, 0.9727(6) for frequencies between 1000 - 2000 cm⁻¹ and

0.9564(4) for frequencies above 2000 cm^{-1}), our results show a median anharmonicity error of 7.5(5) cm^{-1} (RMSE 28(4) cm^{-1}); far better than the median 15.9(5) cm^{-1} (RMSE 32(4) cm^{-1}) anharmonicity error obtained with a uniform global scaling factor of 0.9617(3). We therefore recommend implementing frequency-range-specific scaling factors in harmonic frequency calculations to achieve superior performance. Future benchmarking studies should seek to determine model chemistry choices whose performance can get as close as possible to the anharmonicity error.

Acknowledgement

This research was undertaken with the assistance of resources from the National Computational Infrastructure (NCI Australia), an NCRIS enabled capability supported by the Australian Government.

The authors declare no conflicts of interest.

Supporting Information Available

The compiled experimental data and calculated harmonic frequencies are presented in the article and within the supplementary information.

Specifically, the VIBFREQ1295 database is provided as a csv file with each row containing specific information for the molecules in the database (e.g., total number of atoms and non-hydrogen atoms, and molecular classification), the experimental fundamental and calculated harmonic frequencies (with vibrational modes descriptions, symmetries, resolution, and references to the original publications), as well as references to the parent databases used in the development of VIBFREQ1295.

We also provide a PDF file detailing the acronyms in the csv file, as well as additional analysis supporting our findings described in the main manuscript.

Alternatively, this data is available through the Harvard DataVerse¹⁴ (<https://doi.org/10.7910/DVN/VLVNU7>).

References

- (1) Bézard, B.; De Bergh, C.; Crisp, D.; Maillard, J. P. The deep atmosphere of Venus revealed by high-resolution nightside spectra. *Nature* **1990**, *345*, 508–511.
- (2) Encrenaz, T.; Drossart, P.; Feuchtgruber, H.; Lellouch, E.; Bézard, B.; Fouchet, T.; Atreya, S. K. The atmospheric composition and structure of Jupiter and Saturn from ISO observations: A preliminary review. *Planetary and Space Science* **1999**, *47*, 1225–1242.
- (3) Krasnopolsky, V. A.; Feldman, P. D. Detection of molecular hydrogen in the atmosphere of Mars. *Science* **2001**, *294*, 1914–1917.
- (4) Tielens, A. G. Interstellar polycyclic aromatic hydrocarbon molecules. *Annual Review of Astronomy and Astrophysics* **2008**, *46*, 289–337.
- (5) McGuire, B. A.; Brandon Carroll, P.; Loomis, R. A.; Finneran, I. A.; Jewell, P. R.; Remijan, A. J.; Blake, G. A. Discovery of the interstellar chiral molecule propylene oxide (CH₃CHCH₂O). *Science* **2016**, *352*, 1449–1452.
- (6) Tennyson, J.; Yurchenko, S. N. ExoMol: Molecular line lists for exoplanet and other atmospheres. *Monthly Notices of the Royal Astronomical Society* **2012**, *425*, 21–33.
- (7) Tennyson, J.; Yurchenko, S. N. High Accuracy Molecular Line Lists for Studies of Exoplanets and Other Hot Atmospheres. *Frontiers in Astronomy and Space Sciences* **2022**, *8*, 218.
- (8) Seager, S.; Bains, W.; Petkowski, J. J. Toward a List of Molecules as Potential Biosignature Gases for the Search for Life on Exoplanets and Applications to Terrestrial Biochemistry. *Astrobiology* **2016**, *16*, 465–485.

- (9) Sousa-Silva, C.; Petkowski, J. J.; Seager, S. Molecular Simulations for the Spectroscopic Detection of Atmospheric Gases. *Physical* **2019**, *21*, 18970–18987.
- (10) Zapata Trujillo, J. C. et al. Computational Infrared Spectroscopy of 958 Phosphorus-Bearing Molecules. *Frontiers in Astronomy and Space Sciences* **2021**, *8*, 639068.
- (11) Zapata Trujillo, J. C.; McKemmish, L. K. Meta-analysis of uniform scaling factors for harmonic frequency calculations. *WIREs Computational Molecular Science* **2021**, e1584.
- (12) Scott, A. P.; Radom, L. Harmonic vibrational frequencies: An evaluation of Hartree-Fock, Møller-Plesset, quadratic configuration interaction, density functional theory, and semiempirical scale factors. *Journal of Physical Chemistry* **1996**, *100*, 16502–16513.
- (13) Pople, J. A.; Scott, A. P.; Wong, M. W.; Radom, L. Scaling Factors for Obtaining Fundamental Vibrational Frequencies and Zero-Point Energies from HF/6–31G* and MP2/6–31G* Harmonic Frequencies. *Israel Journal of Chemistry* **1993**, *33*, 345–350.
- (14) Zapata Trujillo, J.; McKemmish, L. VIBFREQ1295. 2022; <https://doi.org/10.7910/DVN/VLVNU7>.
- (15) Hättig, C.; Tew, D. P.; Köhn, A. Communications: Accurate and efficient approximations to explicitly correlated coupled-cluster singles and doubles, CCSD-F12. *Journal of Chemical Physics* **2010**, *132*, 231102.
- (16) Peterson, K. A.; Adler, T. B.; Werner, H. J. Systematically convergent basis sets for explicitly correlated wavefunctions: The atoms H, He, B-Ne, and Al-Ar. *Journal of Chemical Physics* **2008**, *128*, 084102.
- (17) Hill, J. G.; Peterson, K. A. Correlation consistent basis sets for explicitly correlated wavefunctions: Valence and core-valence basis sets for Li, Be, Na, and Mg. *Physical Chemistry Chemical Physics* **2010**, *12*, 10460–10468.

- (18) Witek, H. A.; Morokuma, K. Systematic study of vibrational frequencies calculated with the self-consistent charge density functional tight-binding method. *Journal of Computational Chemistry* **2004**, *25*, 1858–1864.
- (19) Ünal, Y.; Nassif, W.; Özaydin, B. C.; Sayin, K. Scale factor database for the vibration frequencies calculated in M06-2X, one of the DFT methods. *Vibrational Spectroscopy* **2021**, *112*, 103189.
- (20) Healy, E. F.; Holder, A. An evaluation of AM1 calculated vibrational frequencies. *Journal of Molecular Structure: THEOCHEM* **1993**, *281*, 141–156.
- (21) Kesharwani, M. K.; Brauer, B.; Martin, J. M. Frequency and zero-point vibrational energy scale factors for double-hybrid density functionals (and other selected methods): Can anharmonic force fields be avoided? *Journal of Physical Chemistry A* **2015**, *119*, 1701–1714.
- (22) Alecu, I. M.; Zheng, J.; Zhao, Y.; Truhlar, D. G. Computational Thermochemistry: Scale Factor Databases and Scale Factors for Vibrational Frequencies Obtained from Electronic Model Chemistries. *Journal of Chemical Theory and Computation* **2010**, *6*, 2872–2887.
- (23) Tomita, T.; Sjøgren, C. E.; Klaeboe, P.; Papatheodorou, G. N.; Rytter, E. High-temperature infrared and Raman spectra of aluminium chloride dimer and monomer in the vapour phase. *Journal of Raman Spectroscopy* **1983**, *14*, 415–425.
- (24) Orphal, J. High-resolution spectroscopy and analysis of the ν_3 bands of ClNO (nitrosyl chloride) around 30 μm . *Journal of Quantitative Spectroscopy and Radiative Transfer* **2019**, *230*, 115–119.
- (25) McDonald, J. K.; Kalasinsky, V. F.; Geyer, T. J.; Durig, J. R. High-resolution infrared spectra of the ν_1 , ν_2 , and ν_3 fundamentals of ON³⁵Cl. *Journal of Molecular Spectroscopy* **1988**, *132*, 104–122.

- (26) Fernando, W. T.; Bernath, P. F. Fourier transform spectroscopy of the $A1\Pi-X1\Sigma^+$ transition of BH and BD. *Journal of Molecular Spectroscopy* **1991**, *145*, 392–402.
- (27) Durig, J.; Kim, Y. H.; Guirgis, G.; McDonald, J. FT-Raman and infrared spectra, r_0 structural parameters, ab initio calculations and vibrational assignment for nitril chloride. *Spectrochimica Acta Part A: Molecular Spectroscopy* **1994**, *50*, 463–472.
- (28) Flaud, J. M.; Anantharajah, A.; Tchana, F. K.; Manceron, L.; Orphal, J.; Wagner, G.; Birk, M. High-resolution analysis of the 12.6 μm spectral region of the nitril chloride ClNO₂ molecule. *Journal of Quantitative Spectroscopy and Radiative Transfer* **2019**, *224*, 217–221.
- (29) Anantharajah, A.; Kwabia Tchana, F.; Manceron, L.; Orphal, J.; Flaud, J. M. New analysis of line positions of the ν_3 bands of ³⁵ClNO₂ and ³⁷ClNO₂ around 370 cm^{-1} . *Journal of Quantitative Spectroscopy and Radiative Transfer* **2020**, *253*, 107078.
- (30) Orphal, J.; Morillon-Chapey, M.; Guelachvili, G. The high-resolution infrared spectrum of nitril chloride: Rotational analysis of the ³⁵ClNO₂ ν_4 band around 6 μm . *Journal of Molecular Spectroscopy* **1994**, *165*, 315–322.
- (31) Orphal, J.; Morillon-Chapey, M.; Klee, S.; Mellau, G. C.; Winnewisser, M. The Far-Infrared Spectrum of ClNO₂ Studied by High-Resolution Fourier-Transform Spectroscopy. *Journal of Molecular Spectroscopy* **1998**, *190*, 101–106.
- (32) Bethke, G. W.; Kent Wilson, M.; BETHKEt, O.; KENT WILSONt, M. Vibrational Spectrum of Borine Carbonyl. *The Journal of Chemical Physics* **1957**, *26*, 1118.
- (33) Lambert, L.; Pépin, C.; Cabana, A. High resolution infrared absorption spectrum of borine carbonyl: The analysis of ν_4 and $\nu_4 + \nu_8 - \nu_8$ of ¹¹BH₃CO. *Journal of Molecular Spectroscopy* **1972**, *44*, 578–593.

- (34) Pépin, C.; Lambert, L.; Cabana, A. High-resolution infrared spectrum of borine carbonyl. The ν_7 perpendicular band of $10\text{BH}_3\text{CO}$ at $12\ \mu\text{m}$. *Journal of Molecular Spectroscopy* **1976**, 59, 43–50.
- (35) Drouin, B. J.; Miller, C. E.; Cohen, E. A.; Wagner, G.; Birk, M. Further Investigations of the ClO Rotational Spectrum. *Journal of Molecular Spectroscopy* **2001**, 207, 4–9.
- (36) Melen, F.; Dubois, I.; Bredohl, H. The A-X and B-X transitions of BO . *Journal of Physics B: Atomic and Molecular Physics (1968-1987)* **1985**, 18, 2423.
- (37) Prasad, C. V.; Bernath, P. F. Fourier transform jet-emission spectroscopy of the $\text{A}^2\Pi\text{-X}^2\Sigma^+$ transition of CN . *Journal of Molecular Spectroscopy* **1992**, 156, 327–340.
- (38) Dorofeeva, O. V.; Gurvich, L. V. Ideal Gas Thermodynamic Properties of Sulphur Heterocyclic Compounds. *Journal of Physical and Chemical Reference Data* **1995**, 24, 1351–1375.
- (39) Le Floch, A. Revised molecular constants for the ground state of CO . *Molecular Physics* **1991**, 72, 133–144.
- (40) Hegelund, F.; Larsen, R. W.; Palmer, M. H. High-resolution infrared and theoretical study of gaseous oxazole in the $600\text{--}1400\ \text{cm}^{-1}$ region. *Journal of Molecular Spectroscopy* **2007**, 241, 26–44.
- (41) Mille, G.; Pouchan, C.; Sauvaitre, H.; Chouteau, J. Étude expérimentale et théorique des vibrations moléculaires de l'oxazole. *Journal de Chimie Physique* **1975**, 72, 37–41.
- (42) Miller, C. E.; Brown, L. R. Near infrared spectroscopy of carbon dioxide I. $16\text{O}\ 12\text{C}16\text{O}$ line positions. *Journal of Molecular Spectroscopy* **2004**, 228, 329–354.
- (43) Kauppinen, J.; Jolma, K.; Horneman, V.-M. New wave-number calibration tables for H_2O , CO_2 , and OCS lines between 500 and $900\ \text{cm}^{-1}$. *Applied Optics* **1982**, 21, 3332.
- (44) Robertson, E. G. Vibrational assignment of isoxazole aided by rovibrational data and density functional theory. *Journal of Molecular Spectroscopy* **2005**, 231, 50–56.

- (45) Kwabia Tchana, F.; Lafferty, W. J.; Flaud, J. M.; Manceron, L.; Ndao, M. High-resolution analysis of the ν_1 and ν_5 bands of phosgene $^{35}\text{Cl}_2\text{CO}$ and $^{35}\text{Cl}^{37}\text{ClCO}$. *Molecular Physics* **2015**, *113*, 3241–3246.
- (46) Flaud, J.-M.; Kwabia Tchana, F.; Lafferty, W. J.; Perrin, A.; Manceron, L.; Ndao, M. First far-infrared high-resolution analysis of the ν_2 and ν_4 bands of phosgene $^{35}\text{Cl}_2\text{CO}$ and $^{35}\text{Cl}^{37}\text{ClCO}$. *Molecular Physics* **2017**, *116*, 3463–3467.
- (47) Ndao, M.; Perrin, A.; Kwabia Tchana, F.; Manceron, L.; Flaud, J. M. First far-infrared high resolution analysis of the ν_3 band of phosgene $^{35}\text{Cl}_2\text{CO}$ and $^{35}\text{Cl}^{37}\text{ClCO}$. *Journal of Molecular Spectroscopy* **2016**, *326*, 90–94.
- (48) Flaud, J. M.; Tchana, F. K.; Lafferty, W. J.; Manceron, L.; Ndao, M. First far-infrared high resolution analysis of the ν_6 band of phosgene $^{35}\text{Cl}_2\text{CO}$ and $^{35}\text{Cl}^{37}\text{ClCO}$. *Journal of Molecular Spectroscopy* **2016**, *326*, 87–89.
- (49) Butcher, R. J.; Jones, W. J. Cyclopropane: Studies of some vibration-rotation Raman bands. *Journal of Molecular Spectroscopy* **1973**, *47*, 64–83.
- (50) Masiello, T.; Maki, A.; Blake, T. A. Analysis of the high-resolution infrared spectrum of cyclopropane. *Journal of Molecular Spectroscopy* **2009**, *255*, 45–55.
- (51) Plíva, J.; Merdes, D. W.; Pine, A. S. Parallel bands of cyclopropane in the $3.2\text{-}\mu\text{m}$ region. *Journal of Molecular Spectroscopy* **1992**, *153*, 133–144.
- (52) Merdes, D. W.; Plíva, J.; Pine, A. S. Perpendicular bands of cyclopropane in the $3.5\text{ }\mu\text{m}$ region. *Journal of Molecular Spectroscopy* **1991**, *147*, 431–447.
- (53) Plíva, J.; Terki-Hasseine, M.; Lavorel, B.; Saint-Loup, R.; Santos, J.; Schrötter, H. W.; Berger, H. Inverse Raman spectrum of cyclopropane in the region $3000\text{--}3050\text{ cm}^{-1}$. *Journal of Molecular Spectroscopy* **1989**, *133*, 157–170.

- (54) Perrin, A.; Flaud, J. M.; Bürger, H.; Pawelke, G.; Sander, S.; Willner, H. First high-resolution analysis of the six fundamental bands ν_1 , ν_2 , ν_3 , ν_4 , ν_5 , and ν_6 of COF₃₅Cl in the 340- to 2000-cm⁻¹ region. *Journal of Molecular Spectroscopy* **2001**, 209, 122–132.
- (55) Shaw, R. A.; Castro, C.; Ibrahim, N.; Wieser, H. Vibrational spectra and scaled ab initio harmonic force field for thietane and several deuteriated isotopomers. *Journal of Physical Chemistry* **1988**, 92, 6528–6536.
- (56) McPhail, M. J.; Duxbury, G.; May, R. D. The ν_1 , $2\nu_2$, and $2\nu_3 + \nu_4$ Band System of Carbonyl Fluoride. *Journal of Molecular Spectroscopy* **1997**, 182, 118–123.
- (57) Cohen, E. A.; Drouin, B. J.; Brown, L. R.; Oh, J. J. Terahertz and infrared spectra of carbonyl fluoride, COF₂: Vibration-rotation analyses of the four lowest bands, $2\nu_6$, and ν_6 hot bands; ¹³COF₂ ground state and ν_6 band. *Journal of Quantitative Spectroscopy and Radiative Transfer* **2013**, 114, 13–19.
- (58) Camy-Peyret, C.; Flaud, J. M.; Goldman, A.; Murcray, F. J.; Blatherwick, R. D.; Bonomo, F. S.; Murcray, D. G.; Rinsland, C. P. The ν_4 band of carbonyl fluoride. *Journal of Molecular Spectroscopy* **1991**, 149, 481–490.
- (59) Hewett, K. B.; Shen, M.; Brummel, C. L.; Philips, L. A. High resolution infrared spectroscopy of pyrazine and naphthalene in a molecular beam. *The Journal of Chemical Physics* **1994**, 100, 4077–4086.
- (60) Ram, R. S.; Bernath, P. F.; Davis, S. P. Fourier transform infrared emission spectroscopy of CS. *Journal of Molecular Spectroscopy* **1995**, 173, 146–157.
- (61) Mellouki, A.; Vander Auwera, J.; Demaison, J.; Herman, M. Rotational analysis of the ν_6 band in furan (C₄H₄O). *Journal of Molecular Spectroscopy* **2001**, 209, 136–138.
- (62) Klots, T. D.; Chirico, R. D.; Steele, W. V. Complete vapor phase assignment for the funda-

- mental vibrations of furan, pyrrole and thiophene. *Spectrochimica Acta Part A: Molecular Spectroscopy* **1994**, 50, 765–795.
- (63) Pankoke, B.; Yamada, K. M.; Winnewisser, G. High Resolution I R-Spectra of Furane and Thiophene. *Zeitschrift fur Naturforschung - Section A Journal of Physical Sciences* **1993**, 48, 1193–1202.
- (64) Tokaryk, D. W.; Culligan, S. D.; Billinghurst, B. E.; Van Wijngaarden, J. A. Synchrotron-based far-infrared spectroscopy of furan: Rotational analysis of the ν_{14} , ν_{11} , ν_{18} and ν_{19} vibrational levels. *Journal of Molecular Spectroscopy* **2011**, 270, 56–60.
- (65) Mellouki, A.; Herman, M.; Demaison, J.; Lemoine, B.; Margulès, L. Rotational Analysis of the ν_7 Band in Furan (C₄H₄O). *Journal of Molecular Spectroscopy* **1999**, 198, 348–357.
- (66) Mellouki, A.; Liévin, J.; Herman, M. The vibrational spectrum of pyrrole (C₄H₅N) and furan (C₄H₄O) in the gas phase. *Chemical Physics* **2001**, 271, 239–266.
- (67) Wells, J. S.; Schneider, M.; Maki, A. G. Calibration tables covering the 1460- to 1550-cm⁻¹ region from heterodyne frequency measurements on the ν_3 bands of ¹²CS₂ and ¹³CS₂. *Journal of Molecular Spectroscopy* **1988**, 132, 422–428.
- (68) Blanquet, G.; Baeten, E.; Cauuet, I.; Walrand, J.; Courtoy, C. P. Diode-laser measurements of carbon disulfide and general rovibrational analysis. *Journal of Molecular Spectroscopy* **1985**, 112, 55–70.
- (69) Jolma, K.; Kauppinen, J. High-resolution infrared spectrum of CS₂ in the region of the bending fundamental ν_2 . *Journal of Molecular Spectroscopy* **1980**, 82, 214–219.
- (70) Hegelund, F.; Wugt Larsen, R.; Palmer, M. H. The high-resolution infrared spectrum of pyrrole between 900 and 1500 cm⁻¹ revisited. *Journal of Molecular Spectroscopy* **2008**, 252, 93–97.

- (71) Mellouki, A.; Vander Auwera, J.; Herman, M. Rotation-vibration constants for the ν_1 , ν_{22} , ν_{24} , $\nu_{22} + \nu_{24}$, and ground states in pyrrole ($12C_4H_5N$). *Journal of Molecular Spectroscopy* **1999**, *193*, 195–203.
- (72) Held, A.; Herman, M. High resolution spectroscopic study of the first overtone of the N-H stretch and of the fundamentals of the C-H stretches in pyrrole. *Chemical Physics* **1995**, *190*, 407–417.
- (73) Tokaryk, D. W.; van Wijngaarden, J. A. Fourier transform spectra of the ν_{16} , $2\nu_{16}$, and $2\nu_{16} - \nu_{16}$ bands of pyrrole taken with synchrotron radiation This article is part of a Special Issue on Spectroscopy at the University of New Brunswick in honour of Colan Linton and Ron Lees. *Canadian Journal of Physics* **2009**, *87*, 443–448.
- (74) McKellar, A. R.; Billinghurst, B. E. High-resolution synchrotron infrared spectroscopy of thiophosgene: The ν_2 and ν_4 fundamental bands near 500 cm^{-1} . *Journal of Molecular Spectroscopy* **2010**, *260*, 66–71.
- (75) McKellar, A. R.; Billinghurst, B. E. High-resolution synchrotron infrared spectroscopy of thiophosgene: The ν_1 , ν_5 , $2\nu_4$, and $\nu_2 + 2\nu_6$ bands. *Journal of Molecular Spectroscopy* **2015**, *315*, 24–29.
- (76) Frenzel, C. A.; Blick, K. E.; Bennett, C. R.; Niedenzu, K. Investigations of the Raman and infrared spectra of thiophosgene and polymeric species. *The Journal of Chemical Physics* **1970**, *53*, 198–204.
- (77) Hopper, M. J.; Russell, J. W.; Overend, J. Vibrational intensities—XXVI CSF₂ and CSCl₂. *Spectrochimica Acta Part A: Molecular Spectroscopy* **1972**, *28*, 1215–1224.
- (78) Klots, T. Raman vapor spectrum and vibrational assignment for pyridine. *Spectrochimica Acta Part A: Molecular and Biomolecular Spectroscopy* **1998**, *54*, 1481–1498.

- (79) Martinez, R.; Bermejo, D.; Santos, J.; Cancio, P. High-Resolution Stimulated Raman Spectrum of F₂. *Journal of Molecular Spectroscopy* **1994**, *168*, 343–349.
- (80) Billes, F.; Endrédi, H.; Keresztury, G. Vibrational spectroscopy of triazoles and tetrazole. *Journal of Molecular Structure: THEOCHEM* **2000**, *530*, 183–200.
- (81) Bürger, H.; Schippel, G. FTIR investigation and rovibrational analysis of the ν_2 fundamental of OF₂. *Journal of Molecular Spectroscopy* **1987**, *121*, 238–241.
- (82) Taubmann, G.; Jones, H.; Rudolph, H. D.; Takami, M. Diode laser spectroscopy of the ν_1 $2\nu_2$ Fermi diad of OF₂. *Journal of Molecular Spectroscopy* **1986**, *120*, 90–100.
- (83) Taubmann, G. Diode Laser Spectroscopy of the ν_3 Band of OF₂. *Zeitschrift für Naturforschung - Section A Journal of Physical Sciences* **1987**, *42*, 87–90.
- (84) McNaughton, D. High resolution infrared spectrum and molecular structure of dichloroacetylene. *Structural Chemistry* **1992**, *3*, 245–252.
- (85) Klaboe, P.; Kloster-Jensen, E.; Christensen, D. H.; Johnsen, I. The vibrational spectra of dichloro-, dibromo-, diiodo-, bromochloro- and chloriodoacetylene. *Spectrochimica Acta Part A: Molecular Spectroscopy* **1970**, *26*, 1567–1580.
- (86) O'Hara, T. J.; Nofle, R. E. The vibrational spectrum of thionyl fluoride and its oxygen-18 isotopomer. *Journal of Fluorine Chemistry* **1982**, *20*, 149–156.
- (87) Davies, C. J.; Newnham, D. A.; Smith, D. M. High-resolution Fourier-transform infrared spectroscopy of the ν_2 fundamental band of thionyl fluoride, SOF₂. *Physical Chemistry Chemical Physics* **2003**, *5*, 446–450.
- (88) Vanderauwera, J.; Hurtmans, D.; Carleer, M.; Herman, M. The ν_3 Fundamental in C₂H₂. *Journal of Molecular Spectroscopy* **1993**, *157*, 337–357.
- (89) Hietanen, J.; Kauppinen, J. High-resolution infrared spectrum of acetylene in the region of the bending fundamental ν_5 . *Molecular Physics* **1981**, *42*, 411–423.

- (90) Fast, H.; Welsh, H. High-resolution Raman spectra of acetylene, acetylene-d1, and acetylene-d2. *Journal of Molecular Spectroscopy* **1972**, *41*, 203–221.
- (91) Cole, A.; Isaacson, L.; Lord, R. Two vibration-rotation bands of cyanogen fluoride. *Journal of Molecular Spectroscopy* **1967**, *23*, 86–93.
- (92) Farkhsi, A.; Bredohl, H.; Dubois, I.; Remy, F.; Fayt, A. Fourier transform infrared spectrum of FCN: The 1800-2800 cm⁻¹ spectral range. *Journal of Molecular Spectroscopy* **1997**, *181*, 119–126.
- (93) Jones, H.; Lindenmayer, J.; Takami, M. The ν_1 fundamental and associated hot bands of three isotopic forms of cyanogen fluoride by diode laser spectroscopy. *Journal of Molecular Spectroscopy* **1985**, *113*, 339–354.
- (94) Nemes, L.; Luckhaus, D.; Quack, M.; Johns, J. W. Deperturbation of the low-frequency infrared modes of ketene (CH₂CO). *Journal of Molecular Structure* **2000**, *517-518*, 217–226.
- (95) Duncan, J. L.; Ferguson, A. M.; Harper, J.; Tonge, K. H. A combined empirical-ab initio determination of the general harmonic force field of ketene. *Journal of Molecular Spectroscopy* **1987**, *125*, 196–213.
- (96) Escribano, R.; Doménech, J. L.; Cancio, P.; Ortigoso, J.; Santos, J.; Bermejo, D. The ν_1 band of ketene. *The Journal of Chemical Physics* **1994**, *101*, 937–949.
- (97) Duncan, J. L.; Ferguson, A. M.; Harper, J.; Tonge, K. H.; Hegelund, F. High-resolution infrared rovibrational studies of the A1 species fundamentals of isotopic ketenes. *Journal of Molecular Spectroscopy* **1987**, *122*, 72–93.
- (98) Johns, J. W.; Stone, J. M.; Winnewisser, G. The ground state of ketene. *Journal of Molecular Spectroscopy* **1972**, *42*, 523–535.

- (99) Perrin, A.; Valentin, A.; Daumont, L. New analysis of the $2\nu_4$, $\nu_4+\nu_6$, $2\nu_6$, $\nu_3+\nu_4$, $\nu_3+\nu_6$, ν_1 . *Journal of Molecular Structure* **2006**, 780-781, 28–44.
- (100) Perrin, A.; Keller, F.; Flaud, J. M. New analysis of the ν_2 , ν_3 , ν_4 and ν_6 bands of formaldehyde H₂C₁₆O line positions and intensities in the 5-10 μm spectral region. *Journal of Molecular Spectroscopy* **2003**, 221, 192–198.
- (101) Profeta, L. T.; Sams, R. L.; Johnson, T. J.; Williams, S. D. Quantitative infrared intensity studies of vapor-phase glyoxal, methylglyoxal, and 2,3-butanedione (diacetyl) with vibrational assignments. *Journal of Physical Chemistry A* **2011**, 115, 9886–9900.
- (102) Cole, A. R.; Osborne, G. A. Rotational fine structure of the antisymmetric CH stretching band ν_9 , of glyoxal. *Journal of Molecular Spectroscopy* **1970**, 36, 376–385.
- (103) Wugt Larsen, R.; Hegelund, F.; Ceponkus, J.; Nelander, B. A high-resolution ft-ir study of the fundamental bands ν_6 , ν_{10} , and ν_{11} of trans-glyoxal. *Journal of Molecular Spectroscopy* **2002**, 211, 127–134.
- (104) Cole, A. R.; Osborne, G. A. Vibrational spectra of glyoxal, monodeuteroxyoxal and dideuteroxyoxal. *Spectrochimica Acta Part A: Molecular Spectroscopy* **1971**, 27, 2461–2490.
- (105) Benedict, W. S.; Gailar, N.; Plyler, E. K. Rotation-vibration spectra of deuterated water vapor. *The Journal of Chemical Physics* **1956**, 24, 1139–1165.
- (106) Camy-Peyret, C.; Flaud, J. M. Line positions and intensities in the ν_2 band of H₂16O. *Molecular Physics* **1976**, 32, 523–537.
- (107) Enomoto, S.; Asahina, M. Infrared spectra of vinyl chloride and its deuterated derivatives. *Journal of Molecular Spectroscopy* **1966**, 19, 117–130.
- (108) De Lorenzi, A.; Giorgianni, S.; Bini, R. High-resolution FTIR spectrum of vinyl chloride:

- Rovibrational analysis of the ν_{10} and ν_{11} fundamental bands. *Molecular Physics* **2000**, *98*, 355–362.
- (109) Giorgianni, S.; Stoppa, P.; De Lorenzi, A. Infrared laser spectroscopy of the ν_{u} band of $\text{CH}_2\text{=CH}^{37}\text{Cl}$. *Molecular Physics* **1997**, *92*, 301–306.
- (110) Stoppa, P.; Giorgianni, S.; Ghersetti, S. Infrared measurements and rovibrational study of the ν_7 band of vinyl chloride by diode laser spectroscopy. *Molecular Physics* **1997**, *91*, 215–222.
- (111) Demaison, J.; Møllendal, H.; Perrin, A.; Orphal, J.; Tchana, F. K.; Rudolph, H. D.; Willaert, F. Microwave and high resolution infrared spectra of vinyl chloride, ab initio anharmonic force field and equilibrium structure. *Journal of Molecular Spectroscopy* **2005**, *232*, 174–185.
- (112) Giorgianni, S.; De Lorenzi, A.; Stoppa, P.; Ghersetti, S. Infrared spectrum and rovibrational analysis of the ν_6 band of vinyl chloride by diode laser spectroscopy. *Journal of Molecular Spectroscopy* **1992**, *156*, 373–382.
- (113) Brown, L. R.; Crisp, J. A.; Crisp, D.; Naumenko, O. V.; Smirnov, M. A.; Sinita, L. N.; Perrin, A. The absorption spectrum of H_2S between 2150 and 4260 cm^{-1} : Analysis of the positions and intensities in the first ($2\nu_2$, ν_1 , and ν_3) and second ($3\nu_2$, $\nu_1 + \nu_2$, and $\nu_2 + \nu_3$) triad regions. *Journal of Molecular Spectroscopy* **1998**, *188*, 148–174.
- (114) Ulenikov, O. N.; Malikova, A. B.; Koivusaari, M.; Alanko, S.; Anttila, R. High resolution vibrational-rotational spectrum of H_2S in the region of the ν_2 fundamental band. *Journal of Molecular Spectroscopy* **1996**, *176*, 229–235.
- (115) Parellada, R.; Perez-Peña, J.; Arenas, J. F. Infrared spectrum of acetonitrile- ^{15}N . *Journal of Molecular Structure* **1979**, *51*, 1–7.

- (116) Parekunnel, T.; Hirao, T.; Le Roy, R. J.; Bernath, P. F. FTIR Emission Spectra and Molecular Constants for DCl. *Journal of Molecular Spectroscopy* **1999**, *195*, 185–191.
- (117) Williams, R. L. Infrared Spectrum of Methyl Isocyanide. *The Journal of Chemical Physics* **1956**, *25*, 656.
- (118) He, C.; Bernheim, R. High-resolution spectroscopy of methyl isocyanide: The ν_4 fundamental and ground state constants. *Journal of Molecular Spectroscopy* **1992**, *155*, 365–383.
- (119) Le, L.; Pliva, J.; Gold, L.; Bernheim, R. High-Resolution Infrared Spectroscopy of Methyl Isocyanide: The ν_3 , ν_6 , and $\nu_7 + \nu_8$ Bands. *Journal of Molecular Spectroscopy* **1995**, *170*, 506–515.
- (120) Khlifi, M.; Paillous, P.; Bruston, P.; Raulin, F.; Guillemin, J. C. Absolute IR band intensities of CH_2N_2 , CH_3N_3 , and CH_3NC in the 250–4300 cm^{-1} region and upper limits of abundance in Titan’s stratosphere. *Icarus* **1996**, *124*, 318–328.
- (121) Maki, A. G.; Mellau, G. C.; Klee, S.; Winnewisser, M.; Quapp, W. High-temperature infrared measurements in the region of the bending fundamental of $\text{H}^{12}\text{C}^{14}\text{N}$, $\text{H}^{12}\text{C}^{15}\text{N}$, and $\text{H}^{13}\text{C}^{14}\text{N}$. *Journal of Molecular Spectroscopy* **2000**, *202*, 67–82.
- (122) Berney, C. V.; Cormier, A. D. Vibrational spectra of acetyl fluoride and acetyl fluoride- d_3 . *Spectrochimica Acta Part A: Molecular Spectroscopy* **1972**, *28*, 1813–1822.
- (123) Dane, C. B.; Lander, D. R.; Curl, R. F.; Tittel, F. K.; Guo, Y.; Ochsner, M. I.; Moore, C. B. Infrared flash kinetic spectroscopy of HCO. *The Journal of Chemical Physics* **1988**, *88*, 2121–2128.
- (124) Brown, J. M.; Dumper, K.; Lowe, R. S. Further measurement and analysis of lines in the LMR spectrum of HCO at 5.3 μm . *Journal of Molecular Spectroscopy* **1983**, *97*, 441–448.
- (125) Johns, J. W.; McKellar, A. R.; Riggin, M. Laser magnetic resonance spectroscopy of the

- v3 fundamental band of HO₂ at 9.1 μm . *The Journal of Chemical Physics* **1978**, 68, 3957–3966.
- (126) Hollenstein, H.; Günthard, H. H. Solid state and gas infrared spectra and normal coordinate analysis of 5 isotopic species of acetaldehyde. *Spectrochimica Acta Part A: Molecular Spectroscopy* **1971**, 27, 2027–2060.
- (127) Andrews, A. M.; Tretyakov, M. Y.; Pate, B. H.; Fraser, G. T.; Kleiner, I. Fourier-transform infrared and jet-cooled diode-laser spectra of the 867 cm^{-1} v₉ band of acetaldehyde. *Molecular Physics* **1995**, 84, 201–210.
- (128) Herman, M.; Herregodts, F.; Georges, R.; Hepp, M.; Hadj Bachir, I.; Lecoutre, M.; Kleiner, I. Spectroscopic investigation of vibration-rotation bands in acetaldehyde:: Focus on the n v₃ (n=1-5) aldehyde CH stretch bands. *Chemical Physics* **1999**, 246, 433–443.
- (129) Hollenstein, H. Coriolis resonance in cs-asymmetric tops analysis of the v₅, v₁₂- and v₈, v₁₃-coriolis resonance bands in the infrared spectrum of acetaldehyde. *Molecular Physics* **1980**, 39, 1013–1033.
- (130) Kleiner, I.; Herman, M. The fundamental v₁₄ band of acetaldehyde. *Journal of Molecular Spectroscopy* **1994**, 167, 300–313.
- (131) Steiner, D. A.; Polo, S. R.; McCubbin, T. K.; Wishah, K. A. Infrared spectrum of the fundamental v₂ of isocyanic acid. *Journal of Molecular Spectroscopy* **1983**, 98, 453–483.
- (132) Yamada, K. M.; Winnewisser, M.; Johns, J. W. High-resolution spectrum of the v₁ fundamental band of isocyanic acid, HNCO. *Journal of Molecular Spectroscopy* **1990**, 140, 353–372.
- (133) Brown, S. S.; Berghout, H. L.; Crim, F. F. Raman spectroscopy of the N–C–O symmetric (v₃) and antisymmetric (v₂) stretch fundamentals in HNCO. *The Journal of Chemical Physics* **1997**, 107, 9764–9771.

- (134) Steiner, D. A.; Wishah, K. A.; Polo, S. R.; McCubbin, T. K. Infrared spectrum of isocyanic acid between 465 and 1100 cm⁻¹. *Journal of Molecular Spectroscopy* **1979**, 76, 341–373.
- (135) Chao, J.; Hall, K. R.; Marsh, K. N.; Wilhoit, R. C. Thermodynamic Properties of Key Organic Oxygen Compounds in the Carbon Range C1 to C4. Part 2. Ideal Gas Properties. *Journal of Physical and Chemical Reference Data* **1986**, 15, 1369 – 1436.
- (136) Petersen, J. C.; Vervloet, M. Infrared emission spectrum of HNO: The ν_1 band. *Chemical Physics Letters* **1987**, 141, 499–502.
- (137) Johns, J. W.; McKellar, A. R. Laser Stark spectroscopy of the fundamental bands of HNO (ν_2 and ν_3) and DNO (ν_1 and ν_2). *The Journal of Chemical Physics* **1977**, 66, 1217.
- (138) Haurie, M.; Novak, A. Spectres de vibration des molécules CH₃COOH, CH₃COOD, CD₃COOH et CD₃COOD. *Journal de Chimie Physique* **1965**, 62, 137–145.
- (139) Havey, D. K.; Feierabend, K. J.; Black, J. C.; Vaida, V. Temperature-dependent infrared spectra of torsional vibrations in acetic acid. *Journal of Molecular Spectroscopy* **2005**, 229, 151–157.
- (140) Tan, T.; Looi, E.; Lua, K. Improved spectroscopic constants for the ν_2 infrared band of HNO₃. *Journal of Molecular Spectroscopy* **1992**, 155, 420–423.
- (141) Tan, T. L.; Wang, W. F.; Looi, B. C.; Ong, P. P. High resolution FTIR spectrum of the ν_6 band of HNO₃. *Spectrochimica Acta - Part A Molecular Spectroscopy* **1996**, 52, 1315–1317.
- (142) Perrin, A. Recent progress in the analysis of HNO₃ spectra. *Spectrochimica Acta Part A: Molecular and Biomolecular Spectroscopy* **1998**, 54, 375–393.
- (143) Looi, E. C.; Lan, T. L.; Wang, W. F.; Ong, P. P. Improved spectroscopic constants for the ν_7 and ν_8 bands of HNO₃. *Journal of Molecular Spectroscopy* **1996**, 176, 222–225.
- (144) Perrin, A. New analysis of the ν_3 and ν_4 bands of HNO₃ in the 7.6 μm region. *Journal of Physical Chemistry A* **2013**, 117, 13236–13248.

- (145) Perrin, A.; Orphal, J.; Flaud, J. M.; Klee, S.; Mellau, G.; Mäder, H.; Walbrodt, D.; Winnewisser, M. New analysis of the ν_5 and 2 ν_9 bands of HNO_3 by infrared and millimeter wave techniques: Line positions and intensities. *Journal of Molecular Spectroscopy* **2004**, 228, 375–391.
- (146) Goldman, A.; Burkholder, J. B.; Howard, C. J.; Escribano, R.; Maki, A. G. Spectroscopic constants for the ν_9 infrared band of HNO_3 . *Journal of Molecular Spectroscopy* **1988**, 131, 195–200.
- (147) Dinu, D. F.; Ziegler, B.; Podewitz, M.; Liedl, K. R.; Loerting, T.; Grothe, H.; Rauhut, G. The interplay of VSCF/VCI calculations and matrix-isolation IR spectroscopy – Mid infrared spectrum of $\text{CH}_3\text{CH}_2\text{F}$ and $\text{CD}_3\text{CD}_2\text{F}$. *Journal of Molecular Spectroscopy* **2020**, 367, 111224.
- (148) Yamada, C.; Endo, Y.; Hirota, E. Difference frequency laser spectroscopy of the ν_1 band of the HO_2 radical. *The Journal of Chemical Physics* **1998**, 78, 4379.
- (149) Nelson, D. D.; Zahniser, M. S. Diode laser spectroscopy of the ν_3 vibration of the HO_2 radical. *Journal of Molecular Spectroscopy* **1991**, 150, 527–534.
- (150) Burkholder, J. B.; Hammer, P. D.; Howard, C. J.; Towle, J. P.; Brown, J. M. Fourier transform spectroscopy of the ν_2 and ν_3 bands of HO_2 . *Journal of Molecular Spectroscopy* **1992**, 151, 493–512.
- (151) Lattanzi, F.; Di Lauro, C.; Vander Auwera, J. Toward the understanding of the high resolution infrared spectrum of C_2H_6 near $3.3\ \mu\text{m}$. *Journal of Molecular Spectroscopy* **2011**, 267, 71–79.
- (152) Borvayeh, L.; Moazzen-Ahmadi, N.; Horneman, V. M. The ν_{12} - ν_9 band of ethane: A global frequency analysis of data from the four lowest vibrational states. *Journal of Molecular Spectroscopy* **2008**, 250, 51–56.

- (153) Helvoort, V. K.; Fantoni, R.; Knippers, W.; Stolte, S. The Raman spectrum of ethane from 600 to 6500 cm⁻¹ Stokes shifts. *Chemical Physics* **1987**, *111*, 445–465.
- (154) Lattanzi, F.; Di Lauro, C.; Horneman, V. M. High resolution difference bands of ethane C₂H₆ from torsionally excited lower states: Rotation-torsion structure of the ν_2 , ν_{11} and $\nu_4 + \nu_{11}$ vibrational states. *Molecular Physics* **2011**, *109*, 2375–2383.
- (155) Moazzen-Ahmadi, N.; Oliaee, J. N. The band system of ethane around 7 micron: Frequency analysis of the ν_6 band. *Journal of Quantitative Spectroscopy and Radiative Transfer* **2016**, *180*, 7–13.
- (156) Lafferty, W. J.; Olson, W. B. The high-resolution infrared spectra of the ν_2 and ν_3 bands of HOCl. *Journal of Molecular Spectroscopy* **1986**, *120*, 359–373.
- (157) Wells, J. S.; Sams, R. L.; Lafferty, W. J. The High Resolution Infrared Spectrum of the ν_1 Band of HOCl. *Journal of Molecular Spectroscopy* **1979**, *77*, 349 – 364.
- (158) Kutzer, P.; Weismann, D.; Waßmuth, B.; Pirali, O.; Roy, P.; Yamada, K. M.; Giesen, T. F. Far-infrared spectra of dimethyl-ether and its ¹³C enriched isotopologues: The fundamental band of the C–O–C in plane bending mode, ν_7 . *Journal of Molecular Spectroscopy* **2016**, *329*, 28–34.
- (159) Coudert, L. H.; Çarçabal, P.; Chevalier, M.; Broquier, M.; Hepp, M.; Herman, M. High-resolution analysis of the ν_6 , ν_{17} , and ν_{21} bands of dimethyl ether. *Journal of Molecular Spectroscopy* **2002**, *212*, 203–207.
- (160) Perchard, J.-P.; Forel, M.-T.; Josien, M.-L. Étude par spectroscopie infrarouge de quelques molécules gem-diméthylées. *Journal de Chimie Physique* **1964**, *61*, 632–644.
- (161) Bürger, H.; Pawelke, G.; Sommer, S.; Rahner, A.; Appelman, E.; Mills, I. The high-resolution infrared spectrum of HOF near 2700 cm⁻¹: The ground and $2\nu_2$ states. *Journal of Molecular Spectroscopy* **1989**, *136*, 197–204.

- (162) Bürger, H.; Pawelke, G.; Rahner, A.; Appelman, E.; Mills, I. The infrared spectrum of the ν_2 and ν_3 bands of H₁₆OF, H₁₈OF, and D₁₆OF. *Journal of Molecular Spectroscopy* **1988**, *128*, 278–287.
- (163) Ellwood, J. A.; Steele, D.; Gerrard, D. Vibrational absorption intensities in chemical analysis—VIII. Dimethyl sulphide. *Spectrochimica Acta Part A: Molecular Spectroscopy* **1994**, *50*, 913–928.
- (164) Jabri, A.; Belkhodja, Y.; Berger, Y.; Kleiner, I.; Asselin, P. High resolution rovibrational analysis of dimethyl sulfide spectrum in the 10 μm atmospheric window combining supersonic jet-quantum cascade laser and FTIR spectroscopies. *Journal of Molecular Spectroscopy* **2018**, *349*, 32–36.
- (165) King, S. T.; Overend, J. Infrared and Raman spectra of trans N₂F₂. *Spectrochimica Acta* **1966**, *22*, 689–694.
- (166) Hore, N. R.; Russell, D. K.; Wesendrup, R. High-resolution tunable diode laser study of the ν_2 band system of monochloroacetylene. *Journal of Molecular Spectroscopy* **2002**, *213*, 153–157.
- (167) Nela, M.; Niskanen, K.; Vaittinen, O.; Halonen, L.; Bürger, H.; Polanz, O. High-resolution infrared and laser photoacoustic spectroscopy of monochloroacetylene. *Molecular Physics* **2002**, *100*, 655–665.
- (168) Giguère, P. A.; Liu, I. D. On the Infrared Spectrum of Hydrazine. *The Journal of Chemical Physics* **1952**, *20*, 136.
- (169) Durig, J. R.; Griffin, M. G.; Macnamee, R. W. Raman spectra of gases. XV: Hydrazine and hydrazine-d₄. *Journal of Raman Spectroscopy* **1975**, *3*, 133–141.
- (170) Yamaguchi, A.; Ichishima, I.; Shimanouchi, T.; Mizushima, S.-I. Far infra-red spectrum of hydrazine. *Spectrochimica Acta* **1960**, *16*, 1471–1485.

- (171) Holland, J. K.; Newnham, D. A.; Mills, I. M.; Herman, M. Vibration-rotation spectra of monofluoroacetylene: 1700 to 7500 cm⁻¹. *Journal of Molecular Spectroscopy* **1992**, *151*, 346–368.
- (172) Ting, W.-J.; Chang, C.-H.; Chen, S.-E.; Chen, H.-C.; Shy, J.-T.; Drouin, B. J.; Daly, A. M. Precision frequency measurement of N₂O transitions near 45 μ m and above 150 μ m. *Journal of the Optical Society of America B* **2014**, *31*, 1954.
- (173) Horneman, V. M. High accurate peak positions for calibration purposes with the lowest fundamental bands ν_2 of N₂O and CO₂. *Journal of Molecular Spectroscopy* **2007**, *241*, 45–50.
- (174) AlSaif, B.; Lamperti, M.; Gatti, D.; Laporta, P.; Fermann, M.; Farooq, A.; Lyulin, O.; Campargue, A.; Marangoni, M. High accuracy line positions of the ν_1 fundamental band of ¹⁴N ²¹⁶O. *Journal of Quantitative Spectroscopy and Radiative Transfer* **2018**, *211*, 172–178.
- (175) Maki, A. G. High-resolution infrared spectrum of cyanogen. *Journal of Molecular Spectroscopy* **2011**, *269*, 166–174.
- (176) Hirschmann, R. P.; Anderson, L. R.; Harnish, D. F.; Fox, W. B. The infrared spectrum of dichlorofluoroamine, NFCl₂. *Spectrochimica Acta* **1968**, *24A*, 1267 – 1270.
- (177) Evans, J. C.; Nyquist, R. A. The vibrational spectra and vibrational assignments of the propargyl halides. *Spectrochimica Acta* **1963**, *19*, 1153–1163.
- (178) Ettinger, R. Infrared spectrum of chlorodifluoroamine, ClNF₂. *The Journal of Chemical Physics* **1963**, *38*, 2427–2429.
- (179) Comeford, J. J. Vibrational Spectrum of ClNF₂. *The Journal of Chemical Physics* **1966**, *45*, 3463–3465.

- (180) Bolotova, I. B.; Ulenikov, O. N.; Bekhtereva, E. S.; Albert, S.; Bauerecker, S.; Hollenstein, H.; Lerch, P.; Quack, M.; Peter, T.; Seyfang, G.; Wokaun, A. High resolution analysis of the FTIR spectra of trifluoroamine NF₃. *Journal of Molecular Spectroscopy* **2018**, *348*, 87–102.
- (181) Najib, H. Experimental values of the rotational and vibrational constants and equilibrium structure of nitrogen trifluoride. *Journal of Molecular Spectroscopy* **2015**, *312*, 1–5.
- (182) Kisiel, Z.; Martin-Drumel, M. A.; Pirali, O. Lowest vibrational states of acrylonitrile from microwave and synchrotron radiation spectra. *Journal of Molecular Spectroscopy* **2015**, *315*, 83–91.
- (183) Khlifi, M.; Nollet, M.; Paillous, P.; Bruston, P.; Raulin, F.; Bénilan, Y.; Khanna, R. K. Absolute Intensities of the Infrared Bands of Gaseous Acrylonitrile. *Journal of Molecular Spectroscopy* **1999**, *194*, 206–210.
- (184) Ram, R. S.; Bernath, P. F.; Hinkle, K. H. Infrared emission spectroscopy of NH: Comparison of a cryogenic echelle spectrograph with a Fourier transform spectrometer. *Journal of Chemical Physics* **1999**, *110*, 5557–5563.
- (185) Nissen, S.; Hegelund, F.; Johnson, M. S.; Nelander, B. High-resolution infrared study of the ν_{11} band of allene. *Journal of Molecular Spectroscopy* **2002**, *216*, 197–202.
- (186) Plíva, J.; Martin, C. The spectrum of allene near 5 μm . *Journal of Molecular Spectroscopy* **1982**, *91*, 218–237.
- (187) Es-Sebbar, E.; Jolly, A.; Benilan, Y.; Farooq, A. Quantitative mid-infrared spectra of allene and propyne from room to high temperatures. *Journal of Molecular Spectroscopy* **2014**, *305*, 10–16.
- (188) Maki, A. G.; Pine, A. S.; Dang-Nhu, M. A Doppler-limited study of the infrared spectrum of allene from 2965 to 3114 cm^{-1} . *Journal of Molecular Spectroscopy* **1985**, *112*, 459–481.

- (189) Ohshima, Y.; Yamamoto, S.; Kuchitsu, K.; Nakanaga, T.; Takeo, H.; Matsumura, C. Diode laser spectrum of the $\nu_7 \nu_9 + \nu_{11}$ band system of allene. *Journal of Molecular Spectroscopy* **1986**, *117*, 138–151.
- (190) Hegelund, F. Reanalysis of the ν_9 , ν_{10} band system in allene. *Journal of Molecular Spectroscopy* **1994**, *165*, 586–587.
- (191) Urban, S.; Spirko, V.; Papousek, D.; Kauppinen, J.; Belov, S. P.; Gershtein, L. I.; Krupnov, A. F. A simultaneous analysis of the microwave, submillimeterwave, far infrared, and infrared-microwave two-photon transitions between the ground and ν_2 inversion-rotation levels of $^{14}\text{NH}_3$. *Journal of Molecular Spectroscopy* **1981**, *88*, 274–292.
- (192) Kleiner, I.; Brown, L. R.; Tarrago, G.; Kou, Q. L.; Picqué, N.; Guelachvili, G.; Dana, V.; Mandin, J. Y. Positions and intensities in the $2\nu_4/\nu_1/\nu_3$ vibrational system of $^{14}\text{NH}_3$ near $3 \mu\text{m}$. *Journal of Molecular Spectroscopy* **1999**, *193*, 46–71.
- (193) Cottaz, C.; Kleiner, I.; Tarrago, G.; Brown, L. R.; Margolis, J. S.; Poynter, R. L.; Pickett, H. M.; Fouchet, T.; Drossart, P.; Lellouch, E. Line positions and intensities in the $2\nu_2/\nu_4$ vibrational system of $^{14}\text{NH}_3$ near $5\text{--}7 \mu\text{m}$. *Journal of Molecular Spectroscopy* **2000**, *203*, 285–309.
- (194) Kerstel, E. R.; Lehmann, K. K.; Pate, B. H.; Scoles, G. Reinvestigation of the acetylenic C-H stretching fundamental of propyne via high resolution, optothermal infrared spectroscopy: Nonresonant perturbations to ν_1 . *The Journal of Chemical Physics* **1994**, *100*, 2588–2595.
- (195) Go, J.; Cronin, T. J.; Perry, D. S. A free-jet infrared double resonance study of the threshold region of IVR. The ν_6 , $\nu_1 + \nu_6$, and $2\nu_1$ bands of propyne. *Chemical Physics* **1993**, *175*, 127–145.
- (196) Pracna, P.; Muller, H. S.; Klee, S.; Horneman, V. M. Interactions in symmetric top molecules between vibrational polyads: Rotational and rovibrational spectroscopy of low-lying states of propyne, $\text{H}_3\text{C-CCH}$. *Molecular Physics* **2004**, *102*, 1555–1568.

- (197) Henfrey, N. F.; Thrush, B. A. A high-resolution study of the ν_3 and $2\nu_{80}$ bands of propyne. *Journal of Molecular Spectroscopy* **1987**, *121*, 150–166.
- (198) Pracna, P.; Müller, H.; Urban, S.; Horneman, V.-M.; Klee, S. Interactions between vibrational polyads of propyne, H_3CCCH : Rotational and rovibrational spectroscopy of the levels around 1000cm^{-1} . *Journal of Molecular Spectroscopy* **2009**, *256*, 152–162.
- (199) Henfrey, N. F.; Thrush, B. A. A high-resolution study of the ν_7 band of propyne. *Journal of Molecular Spectroscopy* **1985**, *113*, 426–450.
- (200) Comeford, J. J.; Mann, D. E.; Schoen, L. J.; Lide, D. R. Infrared spectrum of difluoramine. *The Journal of Chemical Physics* **1963**, *38*, 461–463.
- (201) McKellar, A. R.; Billinghurst, B. E.; Xu, L. H.; Lees, R. M. High-resolution synchrotron infrared spectroscopy of acrolein: The interacting 101 and 141181 states and other vibrational levels between 1020 and 1200 cm^{-1} . *Journal of Molecular Spectroscopy* **2018**, *350*, 51–56.
- (202) Hamada, Y.; Nishimura, Y.; Tsuboi, M. Infrared spectrum of trans-acrolein. *Chemical Physics* **1985**, *100*, 365–375.
- (203) McKellar, A. R.; Billinghurst, B. E.; Xu, L. H.; Lees, R. M. High-resolution synchrotron infrared spectroscopy of acrolein: The vibrational levels between 850 and 1020 cm^{-1} . *Journal of Molecular Spectroscopy* **2015**, *317*, 16–25.
- (204) McKellar, A. R.; Tokaryk, D. W.; Appadoo, D. R. The far-infrared spectrum of acrolein, CH_2CHCHO : The ν_{18} fundamental and $(\nu_{17} + \nu_{18}) - \nu_{18}$ hot bands. *Journal of Molecular Spectroscopy* **2007**, *244*, 146–152.
- (205) McKellar, A. R.; Appadoo, D. R. High-resolution synchrotron far-infrared spectroscopy of acrolein: The vibrational levels below 700 cm^{-1} . *Journal of Molecular Spectroscopy* **2008**, *250*, 106–113.

- (206) Perrin, A.; Flaud, J. M.; Goldman, A.; Camy-Peyret, C.; Lafferty, W. J.; Arcas, P.; Rinsland, C. P. NO₂ and SO₂ line parameters: 1996 HITRAN update and new results. *Journal of Quantitative Spectroscopy and Radiative Transfer* **1998**, *60*, 839–850.
- (207) Ainetschian, A.; Fraser, G. T.; Ortigoso, J.; Pate, B. H. Contaminated torsional tunneling splittings in five normal-mode vibrations of propene. *The Journal of Chemical Physics* **1994**, *100*, 729–732.
- (208) Silvi, B.; Labarbe, P.; Perchard, J. P. Spectres de vibration et coordonnées normales de quatre espèces isotopiques de propène. *Spectrochimica Acta Part A: Molecular Spectroscopy* **1973**, *29*, 263–276.
- (209) Lafferty, W. J.; Flaud, J. M.; Herman, M. Resolved torsional splitting in the ν_{18} and ν_{19} -bands of propene. *Journal of Molecular Structure* **2006**, *780-781*, 65–69.
- (210) Es-sebbar, E. t.; Alrefae, M.; Farooq, A. Infrared cross-sections and integrated band intensities of propylene: Temperature-dependent studies. *Journal of Quantitative Spectroscopy and Radiative Transfer* **2014**, *133*, 559–569.
- (211) Sung, K.; Toon, G. C.; Drouin, B. J.; Mantz, A. W.; Smith, M. A. H. FT-IR measurements of cold propene (C₃H₆) cross-sections at temperatures between 150 and 299 K. *Journal of Quantitative Spectroscopy and Radiative Transfer* **2018**, *213*, 119–132.
- (212) Müller, A.; Mohan, N.; Cyvin, S. J.; Weinstock, N.; Glemser, O. Molecular constants for NSCl and NSF. *Journal of Molecular Spectroscopy* **1976**, *59*, 161–170.
- (213) Robertson, E. G.; McNaughton, D. Maximising rovibrational assignments in the ν_1 band of NSCl by spectral analysis by subtraction of simulated intensities (SASSI). *Journal of Molecular Spectroscopy* **2006**, *238*, 56–63.
- (214) Flaud, J. M.; Lafferty, W. J.; Herman, M. First high resolution analysis of the absorption

- spectrum of propane in the 6.7 μm to 7.5 μm spectral region. *Journal of Chemical Physics* **2001**, *114*, 9361–9366.
- (215) Gayles, J. N.; King, W. T. The infrared spectrum of propane. *Spectrochimica Acta* **1965**, *21*, 543–557.
- (216) Grant, D. M.; Pugmire, R. J.; Livingston, R. C.; Strong, K. A.; McMurtry, H. L.; Brugger, R. M. Methyl Libration in Propane Measured with Neutron Inelastic Scattering. *The Journal of Chemical Physics* **1970**, *52*, 4418–4423.
- (217) Kwabia Tchana, F.; Flaud, J. M.; Lafferty, W. J.; Manceron, L.; Roy, P. The first high-resolution analysis of the low-lying ν_9 band of propane. *Journal of Quantitative Spectroscopy and Radiative Transfer* **2010**, *111*, 1277–1281.
- (218) Flaud, J. M.; Tchana, F. K.; Lafferty, W. J.; Nixon, C. A. High resolution analysis of the ν_{26} and $2\nu_9$ - ν_9 bands of propane: Modelling of Titan's infrared spectrum at 13.4 μm . *Molecular Physics* **2010**, *108*, 699–704.
- (219) Perrin, A.; Flaud, J. M.; Kwabia-Tchana, F.; Manceron, L.; Groner, P. Investigation of the ν_8 and ν_{21} bands of propane $\text{CH}_3\text{CH}_2\text{CH}_3$ at 11.5 and 10.9 μm : evidence of large amplitude tunnelling effects. *Molecular Physics* **2019**, *117*, 323–339.
- (220) Miller, K.; Emken, W.; Duncan, L. The low temperature infrared spectrum of thiazyl fluoride and the addition compounds of thiazyl fluoride with boron trifluoride, phosphorus pentafluoride and arsenic pentafluoride. *Journal of Fluorine Chemistry* **1984**, *26*, 125–132.
- (221) Lolck, J. E.; Brodersen, S. The ν_2 , $\nu_2 + 2\nu_{70}$, and $2\nu_{70}$ Raman band-accumulations of C_3O_2 . *Journal of Molecular Spectroscopy* **1978**, *72*, 445–462.
- (222) Weber, W. H.; Maker, P. D.; Peters, C. W. Analysis of tunable diode laser spectra of the ν_4 band of $^{12}\text{C}_3^{16}\text{O}_2$. *The Journal of Chemical Physics* **2008**, *64*, 2149.

- (223) Lolck, J. E.; Brodersen, S. Some Raman bands of C₃O₂. *Journal of Molecular Spectroscopy* **1979**, 75, 234–244.
- (224) Fusina, L.; Mills, I. M.; Guelachvili, G. Carbon suboxide: The infrared spectrum from 1800 to 2600 cm⁻¹. *Journal of Molecular Spectroscopy* **1980**, 79, 101–122.
- (225) Auwera, J. V.; Holland, J. K.; Jensen, P.; Johns, J. W. The ν_6 Band System of C₃O₂ Near 540 cm⁻¹. *Journal of Molecular Spectroscopy* **1994**, 163, 529–540.
- (226) Halonen, L.; Mills, I. M.; Kauppinen, J. Vibrational renner-teller effects in the infrared spectrum of carbon suboxide. *Molecular Physics* **1981**, 43, 913–931.
- (227) Vander Auwera, J.; Johns, J. W.; Polyansky, O. L. The far infrared spectrum of C₃O₂. *The Journal of Chemical Physics* **1998**, 95, 2299.
- (228) Wagner, G.; Birk, M.; Schreier, F.; Flaud, J. M. Spectroscopic database for ozone in the fundamental spectral regions. *Journal of Geophysical Research* **2002**, 107, 4626.
- (229) Guelachvili, G.; Craig, A. M.; Ramsay, D. A. High-resolution Fourier studies of diacetylene in the regions of the ν_4 and ν_5 fundamentals. *Journal of Molecular Spectroscopy* **1984**, 105, 156–192.
- (230) McNaughton, D.; Bruget, D. N. The high-resolution infrared spectrum of diacetylene and structures of diacetylene, triacetylene and dicyanoacetylene. *Journal of Molecular Structure* **1992**, 273, 11–25.
- (231) Vander Auwera, J.; Fayt, A. Absolute line intensities for carbonyl sulfide from 827 to 2939 cm⁻¹. *Journal of Molecular Structure* **2006**, 780-781, 134–141.
- (232) Kagann, R. H. Infrared absorption intensities for OCS. *Journal of Molecular Spectroscopy* **1982**, 94, 192–198.

- (233) Krasnoshchekov, S. V.; Craig, N. C.; Boopalachandran, P.; Laane, J.; Stepanov, N. F. Anharmonic Vibrational Analysis of the Infrared and Raman Gas-Phase Spectra of s-trans- and s-gauche-1,3-Butadiene. *Journal of Physical Chemistry A* **2015**, *119*, 10706–10723.
- (234) Halonen, M.; Halonen, L.; Nesbitt, D. J. Structural Issues in Conjugated Hydrocarbons: High-Resolution Infrared Slit-Jet Spectroscopy of trans -1,3-Butadiene. *The Journal of Physical Chemistry A* **2004**, *108*, 3367–3372.
- (235) Craig, N. C.; Davis, J. L.; Hanson, K. A.; Moore, M. C.; Weidenbaum, K. J.; Lock, M. Analysis of the rotational structure in bands in the high-resolution infrared spectra of butadiene and butadiene-2,3-d₂: Refinement in assignments of fundamentals. *Journal of Molecular Structure* **2004**, *695-696*, 59–69.
- (236) Craig, N. C.; Sams, R. L. An investigation of the rotamers of butadiene by high-resolution infrared spectroscopy. *Journal of Physical Chemistry A* **2008**, *112*, 12637–12646.
- (237) Martin-Drumel, M. A.; Porterfield, J. P.; Goubet, M.; Asselin, P.; Georges, R.; Soulard, P.; Nava, M.; Changala, P. B.; Billingham, B.; Pirali, O.; McCarthy, M. C.; Baraban, J. H. Synchrotron-Based High Resolution Far-Infrared Spectroscopy of trans-Butadiene. *Journal of Physical Chemistry A* **2020**, *124*, 2427–2435.
- (238) Evans, C. J.; McNaughton, D.; Dexter, P.; Lawrance, W. High-resolution fourier transform infrared spectroscopy of nitrosyl fluoride. *Journal of Molecular Spectroscopy* **1998**, *187*, 75–81.
- (239) Foster, S. C.; Johns, J. W. High-resolution Fourier transform spectroscopy of the ν_2 and ν_3 fundamentals of nitrosyl fluoride, FNO. *Journal of Molecular Spectroscopy* **1984**, *103*, 176–186.
- (240) Winther, F.; Schönhoff, M. The Fundamental Vibrations of NC–CC–CN (Dicyanoacetylene). *Journal of Molecular Spectroscopy* **1997**, *186*, 54–65.

- (241) Winther, F.; Ketelsen, M.; Guarnieri, A. The infrared and Raman spectrum of dicyanoacetylene. The ν_9 fundamental. *Journal of Molecular Structure* **1994**, 320, 65–73.
- (242) Winther, F.; Ketelsen, M.; Niedenhoff, M.; Yamada, K. M. The ν_4 Rotation Vibration Band of Dicyanoacetylene. *Zeitschrift fur Naturforschung - Section A Journal of Physical Sciences* **1992**, 47, 1253–1254.
- (243) Winther, F.; Schönhoff, M.; LePrince, R.; Guarnieri, A.; Bruget, D. N.; McNaughton, D. The infrared rotation-vibration spectrum of dicyanoacetylene: The ground and $\nu_9 = 1$ state rotational constants. *Journal of Molecular Spectroscopy* **1992**, 152, 205–212.
- (244) Edwards, H. G. Vibrational raman spectrum and force constants of phosphorus, P₄. *Journal of Molecular Structure* **1993**, 295, 95–100.
- (245) Chhiba, M.; Vergotten, G. The structures and vibrational frequencies of a series of linear alkenes obtained using the spectroscopic potential SPASIBA. *Journal of Molecular Structure* **1994**, 326, 35–58.
- (246) Mirri, A. M.; Scappini, F.; Favero, P. G. Millimeter wave spectrum of PF₃ and PCl₃ and force constants determination. *Spectrochimica Acta* **1965**, 21, 965–971.
- (247) Evans, C. J.; Sinik, A.; Medcraft, C.; McNaughton, D.; Appadoo, D.; Robertson, E. G. IR band profiling of dichlorodifluoromethane in the greenhouse window: High-resolution FTIR spectroscopy of ν_2 and ν_8 . *Journal of Physical Chemistry A* **2014**, 118, 2480–2487.
- (248) Giorgianni, S.; Gambi, A.; Baldacci, A.; De Lorenzi, A.; Ghersetti, S. Infrared Study of the ν_1 Band of CF₂Cl₂ by Diode Laser Spectroscopy. *Journal of Molecular Spectroscopy* **1990**, 144, 230–238.
- (249) Giorgianni, S.; Gambi, A.; Franco, L.; Ghersetti, S. Infrared spectrum and molecular force field of CF₂Cl₂. *Journal of Molecular Spectroscopy* **1979**, 75, 389–405.

- (250) Robertson, E. G.; Medcraft, C.; McNaughton, D.; Appadoo, D. The limits of rovibrational analysis: The severely entangled ν_1 polyad vibration of dichlorodifluoromethane in the greenhouse IR window. *Journal of Physical Chemistry A* **2014**, *118*, 10944–10954.
- (251) Jones, H.; Morillon-Chapey, M. The 923-cm⁻¹ band of CF₂Cl₂ (freon 12), studied by infrared-microwave double resonance. *Journal of Molecular Spectroscopy* **1982**, *91*, 87–102.
- (252) Najib, H. Experimental rovibrational constants and equilibrium structure of phosphorus trifluoride. *Journal of Molecular Spectroscopy* **2014**, *305*, 17–21.
- (253) Chakraborty, T.; Verma, A. L. Vibrational spectra of CCl₄: Isotopic components and hot bands. Part I. *Spectrochimica Acta - Part A Molecular and Biomolecular Spectroscopy* **2002**, *58*, 1013–1023.
- (254) Chakraborty, T.; Rai, S. N. Comparative study of infrared and Raman spectra of CCl₄ in vapour and condensed phases: Effect of LO-TO splitting resulting from hetero-isotopic TD-TD interactions. *Spectrochimica Acta - Part A: Molecular and Biomolecular Spectroscopy* **2006**, *65*, 406–413.
- (255) Gaynor, J. D.; Wetterer, A. M.; Valente, E. J.; Mayer, S. G. The ν_3 - ν_4 difference band contribution to the CCl₄ symmetric stretch (ν_1) mode. *Journal of Raman Spectroscopy* **2014**, *46*, 189–193.
- (256) Ram, R. S.; Bernath, P. F. Fourier transform infrared emission spectroscopy of ND and PH. *Journal of Molecular Spectroscopy* **1996**, *176*, 329–336.
- (257) Carlos, M.; Gruson, O.; Richard, C.; Boudon, V.; Rotger, M.; Thomas, X.; Maul, C.; Sydow, C.; Domanskaya, A.; Georges, R.; Soulard, P.; Pirali, O.; Goubet, M.; Asselin, P.; Huet, T. R. High-resolution spectroscopy and global analysis of CF₄ rovibrational bands to model its atmospheric absorption. *Journal of Quantitative Spectroscopy and Radiative Transfer* **2017**, *201*, 75–93.

- (258) Tarrago, G.; Lacome, N.; Lévy, A.; Guelachvili, G.; Bézard, B.; Drossart, P. Phosphine spectrum at 4-5 μm : Analysis and line-by-line simulation of $2\nu_2$, $\nu_2 + \nu_4$, $2\nu_4$, ν_1 , and ν_3 bands. *Journal of Molecular Spectroscopy* **1992**, *154*, 30–42.
- (259) Fusina, L.; Di Lonardo, G. The ν_2 and ν_4 bending fundamentals of phosphine (PH_3). *Journal of Molecular Structure* **2000**, *517-518*, 67–78.
- (260) Zachwieja, M. New Investigations of the $\text{A}^2\Delta\text{-X}^2\Pi$ band system in the CH radical and a new reduction of the vibration-rotation spectrum of CH from the ATMOS spectra. *Journal of Molecular Spectroscopy* **1995**, *170*, 285–309.
- (261) Ahmad, I. K.; Hamilton, P. A. The Fourier Transform Infrared Spectrum of PN . *Journal of Molecular Spectroscopy* **1995**, *169*, 286–291.
- (262) Duncan, J. L.; Nivellini, G. D.; Tullini, F. Methylene chloride: The mid-infrared spectrum of an almost vibrationally unperturbed molecule. *Journal of Molecular Spectroscopy* **1986**, *118*, 145–162.
- (263) Lindner, J.; Niemann, R.; Tiemann, E. Laser spectroscopy of the $\text{b}^3\Sigma\text{-u-x}^3\Sigma\text{-g}$ spectrum of S_2 produced by photodissociation. *Journal of Molecular Spectroscopy* **1994**, *165*, 358–367.
- (264) Vogt, J.; Winnewisser, M.; Yamada, K.; Winnewisser, G. The Fourier transform and diode laser spectrum of the ν_2 band of diazomethane. *Chemical Physics* **1984**, *83*, 309–318.
- (265) Nemes, L.; Vogt, J.; Winnewisser, M. Analysis of the three lowest frequency vibration-rotation bands of diazomethane. *Journal of Molecular Structure* **1990**, *218*, 219–224.
- (266) Moore, C. B.; Pimentel, G. C. Infrared Spectra of Gaseous Diazomethane. *Journal of Chemical Physics* **1964**, *40*, 329 – 341.
- (267) Brown, R. D.; Pez, G. P. Vibrational spectra of thio-thionyl fluoride and difluoro disulphane. *Spectrochimica Acta Part A: Molecular Spectroscopy* **1970**, *26*, 1375–1386.

- (268) Bertie, J. E.; Michaelian, K. H. The Raman spectrum of gaseous acetic acid at 21 °C. *The Journal of Chemical Physics* **1982**, 77, 5267–5271.
- (269) Baskakov, O. I.; Markov, I. A.; Alekseev, E. A.; Motiyenko, R. A.; Lohilahti, J.; Horneman, V. M.; Winnewisser, B. P.; Medvedev, I. R.; Lucia, F. C. Simultaneous analysis of rovibrational and rotational data for the 41, 51, 61, 72, 81, 7191 and 92 states of HCOOH. *Journal of Molecular Structure* **2006**, 795, 54–77.
- (270) Perrin, A.; Vander Auwera, J.; Zelinger, Z. High-resolution Fourier transform study of the ν_3 fundamental band of trans-formic acid. *Journal of Quantitative Spectroscopy and Radiative Transfer* **2009**, 110, 743–755.
- (271) Luo, W.; Zhang, Y.; Li, W.; Duan, C. Jet-cooled infrared absorption spectrum of the ν_4 fundamental band of HCOOH and HCOOD. *Journal of Molecular Spectroscopy* **2017**, 334, 22–25.
- (272) Baskakov, O. I.; Alekseev, E. A.; Motiyenko, R. A.; Lohilahti, J.; Horneman, V. M.; Alanko, S.; Winnewisser, B. P.; Medvedev, I. R.; De Lucia, F. C. FTIR and millimeter wave investigation of the 71 and 91 states of formic acid HCOOH and H¹³COOH. *Journal of Molecular Spectroscopy* **2006**, 240, 188–201.
- (273) Thorwirth, S.; Martin-Drumel, M. A.; Endres, C. P.; Salomon, T.; Zingsheim, O.; Van Wijngaarden, J.; Pirali, O.; Gruet, S.; Lewen, F.; Schlemmer, S.; McCarthy, M. C. An ASAP treatment of vibrationally excited S₂O: The ν_3 mode and the $\nu_3 + \nu_2 - \nu_2$ hot band. *Journal of Molecular Spectroscopy* **2016**, 319, 47–49.
- (274) Lindenmayer, J.; Rudolph, H. D.; Jones, H. The equilibrium structure of disulfur monoxide: Diode laser spectroscopy of ν_1 and ν_3 of S₂¹⁸O and ν_3 of S₂¹⁶O. *Journal of Molecular Spectroscopy* **1986**, 119, 56–67.
- (275) Martin-Drumel, M. A.; Endres, C. P.; Zingsheim, O.; Salomon, T.; Van Wijngaarden, J.; Pirali, O.; Gruet, S.; Lewen, F.; Schlemmer, S.; McCarthy, M. C.; Thorwirth, S. The SOLEIL

- view on sulfur rich oxides: The S₂O bending mode ν_2 at 380 cm⁻¹ and its analysis using an Automated Spectral Assignment Procedure (ASAP). *Journal of Molecular Spectroscopy* **2015**, 315, 72–79.
- (276) Johns, J. W.; Olson, W. B. The infrared spectrum of thioformaldehyde. *Journal of Molecular Spectroscopy* **1971**, 39, 479 – 505.
- (277) McNaughton, D.; Bruget, D. N. Far-Infrared and ν_2 Vibration-Rotation Spectrum of Thioformaldehyde and Infrared Spectrum of Thioglyoxal. *Journal of Molecular Spectroscopy* **1993**, 159, 340–349.
- (278) Flaud, J. M.; Lafferty, W. J.; Perrin, A.; Kim, Y. S.; Beckers, H.; Willner, H. The first high-resolution analysis of the 10- μ m absorption of thioformaldehyde. *Journal of Quantitative Spectroscopy and Radiative Transfer* **2008**, 109, 995–1003.
- (279) Bizzocchi, L.; Cludi, L.; Degli Esposti, C.; Giorgi, A. Millimeter-wave spectroscopy of sulfur dichloride. *Journal of Molecular Spectroscopy* **2000**, 204, 275–280.
- (280) Bray, C.; Perrin, A.; Jacquemart, D.; Lacome, N. The ν_1 , ν_4 and $3\nu_6$ bands of methyl chloride in the 3.4- μ m region: Line positions and intensities. *Journal of Quantitative Spectroscopy and Radiative Transfer* **2011**, 112, 2446–2462.
- (281) Nikitin, A.; Féjard, L.; Champion, J. P.; Bür, H.; Litz, M.; Colmont, J. M.; Bakri, B. New measurements and global analysis of chloromethane in the region from 0 to 1800 cm⁻¹. *Journal of Molecular Spectroscopy* **2003**, 221, 199–212.
- (282) Ram, R. S.; Bernath, P. F.; Engleman, R.; Brault, J. W. Fourier Transform Infrared Emission Spectroscopy of SH. *Journal of Molecular Spectroscopy* **1995**, 172, 34–42.
- (283) Papousek, D.; Papoušková, Z.; Ogilvie, J. F.; Pracna, P.; Civis, S.; Winnewisser, M. Vibration-rotational interactions in the states $\nu_2 = 1$ and $\nu_5 = 1$ of H₃12CF. *Journal of Molecular Spectroscopy* **1992**, 153, 145–166.

- (284) Papousek, D.; Ogilvie, J. F.; Civis, S.; Winnewisser, M. The vibration-rotational bands ν_3 , $2\nu_3 - \nu_3$, and $\nu_3 + \nu_6 - \nu_6$ of H_3^{12}CF . *Journal of Molecular Spectroscopy* **1991**, *149*, 109–124.
- (285) Papousek, D.; Tesar, R.; Pracna, P.; Civis, S.; Winnewisser, M.; Belov, S. P.; Tretyakov, M. Y. High-resolution Fourier transform and submillimeter-wave study of the ν_6 band of $^{12}\text{CH}_3\text{F}$. *Journal of Molecular Spectroscopy* **1991**, *147*, 279–299.
- (286) Champion, J. P.; Robiette, A. G.; Mills, I. M.; Graner, G. Simultaneous analysis of the ν_1 , ν_4 , $2\nu_2$, $\nu_2 + \nu_5$, and $2\nu_5$ infrared bands of $^{12}\text{CH}_3\text{F}$. *Journal of Molecular Spectroscopy* **1982**, *96*, 422–441.
- (287) Bethke, G. W.; Kent Wilson, M. Vibrational Spectrum of Disilane. *The Journal of Chemical Physics* **1957**, *26*, 1107.
- (288) Lattanzi, F.; Di Lauro, C.; Horneman, V. M. Torsional tunneling splittings in the $V_4 = 1$ excited torsional state of Si_2H_6 : Analysis of hot bands accompanying fundamental transitions in the high resolution infrared spectrum. *Molecular Physics* **2005**, *103*, 2655–2663.
- (289) LATTANZI, F.; DI LAURO, C.; HORNEMAN, V.-M. The ν_6 , ν_8 , $3\nu_4 + \nu_{12}$ infrared system of Si_2H_6 under high resolution: rotational and torsional analysis. *Molecular Physics* **2003**, *101*, 2895–2906.
- (290) Lattanzi, F.; Di Lauro, C.; Horneman, V. M. Rotation-torsion analysis of the Si_2H_6 infrared fundamental ν_9 , perturbed by excited torsional levels of the vibrational ground state. *Molecular Physics* **2004**, *102*, 507–512.
- (291) McKean, D. C. On the assignment of SiH and SiD stretching frequencies: A reanalysis of the ν_7 bands of Si_2H_6 and Si_2D_6 and a harmonic local mode force field for disilane. *Spectrochimica Acta Part A: Molecular Spectroscopy* **1992**, *48*, 1335–1345.

- (292) Lattanzi, F.; Di Lauro, C.; Horneman, V. M. The high-resolution infrared spectrum of Si₂H₆: Rotation-torsion analysis of the ν_5 and ν_7 fundamentals, and torsional splittings in the degenerate vibrational states. *Molecular Physics* **2004**, *102*, 757–764.
- (293) Halonen, L.; Duxbury, G. High resolution infrared spectrum of methyleneimine, CH₂NH, in the 3 μ m region. *The Journal of Chemical Physics* **1985**, *83*, 2091–2096.
- (294) Duxbury, G.; Kato, H.; Le Lerre, M. L. Laser Stark and interferometric studies of thioformaldehyde and methyleneimine. *Faraday Discussions of the Chemical Society* **1981**, *71*, 97–110.
- (295) Duxbury, G.; Le Lerre, M. L. Fourier transform infrared spectra of CH₂NH: The ν_5 and ν_6 bands. *Journal of Molecular Spectroscopy* **1982**, *92*, 326–348.
- (296) Halonen, L.; Duxbury, G. The Fourier transform infrared spectrum of methyleneimine in the 10 μ m region. *The Journal of Chemical Physics* **1985**, *83*, 2078–2090.
- (297) Halonen, L.; Duxbury, G. Fourier transform infrared spectrum of CH₂NH: The ν_1 band. *Chemical Physics Letters* **1985**, *118*, 246–251.
- (298) Hirota, E.; Ishikawa, H. The vibrational spectrum and molecular constants of silicon dihydride SiH₂ in the ground electronic state. *The Journal of Chemical Physics* **1999**, *110*, 4254.
- (299) Sztraka, L.; Horneman, V. M. Study of vibration-rotation levels in formamide with high resolution FTIR spectroscopy: The ν_{12} , $2\nu_{12}$, ν_{11} , and ν_9 bands. *Journal of Molecular Spectroscopy* **2009**, *255*, 172–182.
- (300) McNaughton, D.; Evans, C. J.; Lane, S.; Nielsen, C. J. The High-Resolution FTIR Far-Infrared Spectrum of Formamide. *Journal of Molecular Spectroscopy* **1999**, *193*, 104 – 117.
- (301) Christensen, D. H.; Nielsen, O. F. Infrared absorption spectra of SiH₂Cl₂, SiDHCl₂ and SiD₂Cl₂. *Journal of Molecular Spectroscopy* **1968**, *27*, 489–498.

- (302) Amyay, B.; Gardez, A.; Georges, R.; Biennier, L.; Vander Auwera, J.; Richard, C.; Boudon, V. New investigation of the ν_3 C-H stretching region of 12CH_4 through the analysis of high temperature infrared emission spectra. *Journal of Chemical Physics* **2018**, *148*.
- (303) Barrett, D.; Carpenter, J. H. The millimeter-wave spectrum of chlorosilane. *Journal of Molecular Spectroscopy* **1984**, *107*, 153–159.
- (304) Newman, C.; Kenneth O’Loane, J.; Polo, S. R.; Kent Wilson, M. Infrared Spectra and Molecular Structures of SiH_3F , SiH_3Cl , and SiH_3Br . *The Journal of Chemical Physics* **1956**, *25*, 855.
- (305) Twagirayezu, S.; Clasp, T. N.; Perry, D. S.; Neill, J. L.; Muckle, M. T.; Pate, B. H. Vibrational coupling pathways in methanol as revealed by coherence-converted population transfer Fourier transform microwave infrared double-resonance spectroscopy. *Journal of Physical Chemistry A* **2010**, *114*, 6818–6828.
- (306) Escribano, R.; Garcia Hernandez, M.; Butcher, R. J. The infrared spectra of SiH_3F : ν_3 and ν_4 bands. *Journal of Molecular Spectroscopy* **1982**, *95*, 334–349.
- (307) Robiette, A. G.; Cartwright, G. J.; Hoy, A. R.; Mills, I. M. The infra-red spectra of silyl fluoride and silyl fluoride- d_3 . *Molecular Physics* **1971**, *20*, 541–553.
- (308) Lees, R. M.; Xu, L. H.; Billingham, B. E. High-resolution Fourier transform synchrotron spectroscopy of the C–S stretching band of methyl mercaptan, CH_3SH . *Journal of Molecular Spectroscopy* **2016**, *319*, 30–38.
- (309) Lees, R. M.; Xu, L. H.; Twagirayezu, S.; Perry, D. S.; Dawadi, M. B.; Billingham, B. E. FTIR synchrotron spectroscopy of the S–H stretching fundamental of the $12\text{CH}_3\text{SH}$ species of methyl mercaptan. *Molecular Physics* **2018**, *116*, 3554–3563.
- (310) Du, Z.; Li, J.; Gao, H.; Luo, G.; Cao, X.; Ma, Y. Ultrahigh-resolution spectroscopy for

- methyl mercaptan at the ν_2 -band by a distributed feedback interband cascade laser. *Journal of Quantitative Spectroscopy and Radiative Transfer* **2017**, *196*, 123–129.
- (311) Lees, R. M.; Xu, L. H.; Guislain, B. G.; Reid, E. M.; Twagirayezu, S.; Perry, D. S.; Dawadi, M. B.; Thapaliya, B. P.; Billingham, B. E. Torsion-rotation structure and quasi-symmetric-rotor behaviour for the CH₃SH asymmetric CH₃-bending and C-H stretching bands of E parentage. *Journal of Molecular Spectroscopy* **2018**, *343*, 18–27.
- (312) Du, Z.; Zhen, W.; Zhang, Z.; Li, J.; Gao, N. Detection of methyl mercaptan with a 3393-nm distributed feedback interband cascade laser. *Applied Physics B: Lasers and Optics* **2016**, *122*, 1–8.
- (313) Johns, J. W.; Kreiner, W. A.; Susskind, J. Measurement and analysis of the ν_4 band of silane. *Journal of Molecular Spectroscopy* **1976**, *60*, 400–411.
- (314) Wilkinson, G. R.; Kent Wilson, M. Infrared Spectra of Some MH₄ Molecules. *The Journal of Chemical Physics* **2004**, *44*, 3867.
- (315) Cabana, A.; Gray, D. L.; Robiette, A. G.; Pierre, G. Analysis of the ν_3 and ν_1 infra-red bands of SiH₄. *Molecular Physics* **1978**, *36*, 1503–1516.
- (316) Gulaczyk, I.; Kreglewski, M.; Asselin, P.; Pirali, O.; Kleiner, I. The NH₂ scissors band of methylamine. *Canadian Journal of Physics* **2020**, *98*, 560–566.
- (317) Gulaczyk, I.; Kreglewski, M.; Horneman, V. M. The C-N stretching band of methylamine. *Journal of Molecular Spectroscopy* **2011**, *270*, 70–74.
- (318) Gray, A. P.; Lord, R. C. Rotation-vibration spectra of methyl amine and its deuterium derivatives. *The Journal of Chemical Physics* **1957**, *26*, 690–705.
- (319) Gulaczyk, I.; Lodyga, W.; Kreglewski, M.; Horneman, V. M. Reinvestigation of the wagging band of methylamine. *Molecular Physics* **2010**, *108*, 2389–2394.

- (320) Gulaczyk, I.; Kreglewski, M. IR rotational spectrum of methylamine. *Journal of Quantitative Spectroscopy and Radiative Transfer* **2020**, 252, 107097.
- (321) Bürger, H.; Ruoff, A. Schwingungsspektren und kraftkonstanten symmetrischer kreisel-II HSiCl₃ und DSiCl₃. *Spectrochimica Acta Part A: Molecular Spectroscopy* **1970**, 26, 1449–1458.
- (322) Kim, H. W.; Zeroka, D. A theoretical study of methylphosphine CH₃PH₂ and selected isotopomers: vibrational analysis and infrared spectra. *Journal of Molecular Structure: THEOCHEM* **2001**, 571, 59–70.
- (323) Bürger, H.; Mkadmi, E. B.; Demaison, J.; Margulès, L.; Gnida, M. High-Resolution Infrared and Millimeter-Wave Study of the $\nu_3 = 1$ State of HSiF₃ and DSiF₃. *Journal of Molecular Spectroscopy* **2000**, 200, 203–209.
- (324) Gnida, M.; Margulès, L.; Cosléou, J.; Bocquet, R.; Demaison, J.; Mkadmi, E. B.; Bürger, H.; Harder, H.; Mäder, H. Radiofrequency, Centimeter-Wave, Millimeter-Wave, and Infrared Spectra of SiHF₃: Investigation of the Ground, $\nu_4 = 1$, and $\nu_6 = 1$ Vibrational States. *Journal of Molecular Spectroscopy* **2000**, 200, 40–54.
- (325) Harada, K.; Akao, S.; Miyachi, K.; Tanaka, K.; Tanaka, T. CO₂ laser Stark spectroscopy of the ν_4 band of SiHF₃: The C₀ rotational constant and vibrationally induced dipole moment. *The Journal of Chemical Physics* **1992**, 96, 5–12.
- (326) Bürger, H.; Biedermann, S.; Ruoff, A. Schwingungsspektren und Kraftkonstanten symmetrischer Kreisel-V1 1 IV. Mitteilung s. Ref. [1]. Die IR-Spektren von HSiF₃ und DSiF₃. *Spectrochimica Acta Part A: Molecular Spectroscopy* **1971**, 27, 1687–1702.
- (327) Borvayeh, L.; Ozier, I.; Bauder, A.; Moazzen-Ahmadi, N. High resolution infrared spectrum and global analysis of ν_5 , ν_{12} , and $\nu_{12} + \nu_6 - \nu_6$ in CH₃SiH₃. *Journal of Molecular Spectroscopy* **2009**, 255, 122–133.

- (328) Wilde, R. E. The infrared spectrum of CH_3SiH_3 and CH_3SiD_3 . *Journal of Molecular Spectroscopy* **1962**, 8, 427–454.
- (329) Petek, H.; Nesbitt, D. J.; Ogilby, P. R.; Moore, C. B. Infrared flash kinetic spectroscopy: The ν_1 and ν_3 spectra of singlet methylene. *Journal of Physical Chemistry* **1983**, 87, 5367–5371.
- (330) Petek, H.; Nesbitt, D. J.; Darwin, D. C.; Ogilby, P. R.; Moore, C. B.; Ramsay, D. A. Analysis of CH_2 a 1A_1 (1,0,0) and (0,0,1) Coriolis-coupled states, a $1\text{A}_1\text{-XX } 3\text{B}_1$ spin-orbit coupling, and the equilibrium structure of CH_2 a 1A_1 state. *The Journal of Chemical Physics* **1989**, 91, 6566–6578.
- (331) Petek, H.; Nesbitt, D. J.; Bradley Moore, C.; Birss, F. W.; Ramsay, D. A. Visible absorption and magnetic-rotation spectroscopy of 1CH_2 : Analysis of the 1A_1 state and the $1\text{A}_1\text{-}3\text{B}_1$ coupling. *The Journal of Chemical Physics* **1987**, 86, 1189–1205.
- (332) Pracna, P.; Ceausu-Velcescu, A.; Horneman, V. M. The ground and $\nu_6=1$ vibrational levels of $\text{HC } 35\text{Cl } 3$: The first high-resolution analysis of the ν_6 fundamental band. *Journal of Quantitative Spectroscopy and Radiative Transfer* **2012**, 113, 1220–1225.
- (333) Pietilä, J.; Alanko, S.; Horneman, V. M.; Anttila, R. High-resolution infrared studies of ν_1 , $2\nu_1$, and $2\nu_4$ bands of CH_35Cl_3 . *Journal of Molecular Spectroscopy* **2002**, 216, 271–283.
- (334) Pietilä, J.; Horneman, V.; Anttila, R.; Lemoine, B.; Raynaud, F.; Colmont, J. The perpendicular fundamental ν_5 of chloroform $12\text{CH}_35\text{Cl}_3$: High resolution infrared study of the ν_5 band together with the millimetre-wave rotational spectrum. *Molecular Physics* **2000**, 98, 549–557.
- (335) Anttila, R.; Alanko, S.; Horneman, V. M. The C-H bending vibration ν_4 of chloroform $\text{CH } 35\text{Cl}_3$. *Molecular Physics* **2004**, 102, 1537–1542.
- (336) Pasa, R.; Horneman, V. M.; Pietilä, J.; Anttila, R. High-resolution study of the infrared band ν_2 of CH_35Cl_3 . *Chemical Physics Letters* **1995**, 247, 277–282.

- (337) Pietilä, J.; Horneman, V.; Anttila, R. High resolution infrared study of the parallel band ν_3 of chloroform CH_3Cl . *Molecular Physics* **1999**, *96*, 1449–1456.
- (338) Sanz, M. E.; McCarthy, M. C.; Thaddeus, P. Rotational transitions of SO, SiO, and SiS excited by a discharge in a supersonic molecular beam: Vibrational temperatures, Dunham coefficients, Born-Oppenheimer breakdown, and hyperfine structure. *Journal of Chemical Physics* **2003**, *119*, 11715–11727.
- (339) Albert, S.; Bauerecker, S.; Bekhtereva, E. S.; Bolotova, I. B.; Hollenstein, H.; Quack, M.; Ulenikov, O. N. High resolution FTIR spectroscopy of fluoroform CHF_3 and critical analysis of the infrared spectrum from 25 to 1500 cm^{-1} . *Molecular Physics* **2018**, *116*, 1091–1107.
- (340) Dübal, H. R.; Quack, M. Tridiagonal Fermi resonance structure in the IR spectrum of the excited CH chromophore in CF_3H . *The Journal of Chemical Physics* **1984**, *81*, 3779–3791.
- (341) Ceausu-Velcescu, A.; Cosléou, J.; Demaison, J.; Graner, G.; Duxbury, G.; Bürger, H. The $\nu_6 = 1$ state of fluoroform, HCF_3 : Analysis of the rotational and vibrational spectra. *Journal of Molecular Spectroscopy* **2003**, *220*, 291–297.
- (342) Müller, H. S.; Brünken, S. Accurate rotational spectroscopy of sulfur dioxide, SO_2 , in its ground vibrational and first excited bending states, $\nu_2 = 0, 1$, up to 2 THz. *Journal of Molecular Spectroscopy* **2005**, *232*, 213–222.
- (343) Guelachvili, G.; Naumenko, O. V.; Ulenikov, O. N. Analysis of the SO_2 absorption Fourier spectrum in regions 1055 to 2000 and 2200 to 2550 cm^{-1} . *Journal of Molecular Spectroscopy* **1987**, *125*, 128–139.
- (344) Douglas, A. E.; Hoy, A. R. The Resonance Fluorescence Spectrum of Cl_2 in the Vacuum Ultraviolet. *Canadian Journal of Physics* **1975**, *53*, 1965–1975.

- (345) Maki, A.; Blake, T. A.; Sams, R. L.; Vulpanovici, N.; Barber, J.; Chrysostom, E. T.; Masiello, T.; Nibler, J. W.; Weber, A. High-resolution infrared spectra of the ν_2 , ν_3 , ν_4 , and $2\nu_3$ bands of $^{32}\text{S}^{16}\text{O}_3$. *Journal of Molecular Spectroscopy* **2001**, *210*, 240–249.
- (346) Barber, J.; Chrysostom, E. T.; Masiello, T.; Nibler, J. W.; Maki, A.; Weber, A.; Blake, T. A.; Sams, R. L. Analysis of ν_2 , ν_4 infrared hot bands of $^{32}\text{S}^{16}\text{O}_3$: Resolution of the puzzle of the ν_1 CARS spectrum. *Journal of Molecular Spectroscopy* **2002**, *216*, 105–112.
- (347) Rochkind, M. M.; Pimentel, G. C. Infrared spectrum and vibrational assignment for chlorine monoxide, Cl_2O . *The Journal of Chemical Physics* **1965**, *42*, 1361–1368.
- (348) Xu, Y.; McKellar, A. R.; Burkholder, J. B.; Orlando, J. J. High-resolution infrared spectrum of the ν_1 and ν_3 bands of dichlorine monoxide, Cl_2O . *Journal of Molecular Spectroscopy* **1996**, *175*, 68–72.
- (349) Roucou, A.; Dhont, G.; Cuisset, A.; Martin-Drumel, M. A.; Thorwirth, S.; Fontanari, D.; Meerts, W. L. High resolution study of the ν_2 and ν_5 rovibrational fundamental bands of thionyl chloride: Interplay of an evolutionary algorithm and a line-by-line analysis. *The Journal of Chemical Physics* **2017**, *147*, 054303.
- (350) Martin-Drumel, M. A.; Mouret, G.; Pirali, O.; Cuisset, A. High-resolution synchrotron far infrared spectroscopy of thionyl chloride: Analysis of the ν_3 and ν_6 fundamental bands. *Journal of Molecular Spectroscopy* **2015**, *315*, 30–36.
- (351) Martz, D. E.; Lagemann, R. T. Infrared spectra of thionyl chloride and sulfuryl chloride. *The Journal of Chemical Physics* **1954**, *22*, 1193–1195.
- (352) Saouli, A.; Dubois, I.; Blavier, J. F.; Bredhol, H.; Blanquet, G.; Meyer, C.; Meyer, F. Fourier Transform Infrared Spectrum of ClCN : Analysis of the $\nu_1 + \nu_3$, $2\nu_2 + \nu_3$, and Associated Hot Bands. *Journal of Molecular Structure* **1994**, *165*, 349 – 357.

- (353) Mizushima, S.; Shimanouchi, T.; Harada, I.; Abe, Y.; Takeuchi, H. Infrared and Raman Spectra of 1,2-Dichloroethane and its Deuterium Compound in the Gaseous, Liquid, and Solid States. *Canadian Journal of Physics* **1975**, *53*, 2085–2094.
- (354) Burger, H.; Schulz, P.; Jacob, E.; Fahnle, M. The Fourier Transform IR Spectra of ClF and BrF. *Zeitschrift für Naturforschung - Section A Journal of Physical Sciences* **1986**, *41*, 1015–1020.
- (355) Marshall, M. D.; McKellar, A. R. The ν_2 fundamental band of triplet CH₂. *The Journal of Chemical Physics* **1986**, *85*, 3716–3723.
- (356) Jensen, P.; Bunker, P. R. The potential surface and stretching frequencies X3B 1 methylene (CH₂) determined from experiment using the Morse oscillator-rigid bender internal dynamics Hamiltonian. *The Journal of Chemical Physics* **1988**, *89*, 1327–1332.
- (357) Selig, H.; Claassen, H. H.; Holloway, J. H. Infrared and raman spectra of ClF₃ and BrF₃. *The Journal of Chemical Physics* **1970**, *52*, 3517–3521.
- (358) Rusell D., J. I. NIST Computational Chemistry Comparison and Benchmark Database NIST Standard Reference Database Number 101. 2020; <http://cccbdb.nist.gov/>.
- (359) Shimanouchi, T. Tables of molecular vibrational frequencies. Consolidated volume II. *Journal of Physical and Chemical Reference Data* **1977**, *6*, 993–1102.
- (360) Huber, K. P.; Herzberg, G. *Molecular Spectra and Molecular Structure*; Springer US: Boston, MA, 1979; p 716.
- (361) WebBook, N. C. Methylphosphonic Acid. 1966.
- (362) Grimme, S.; Bohle, F.; Hansen, A.; Pracht, P.; Spicher, S.; Stahn, M. Efficient Quantum Chemical Calculation of Structure Ensembles and Free Energies for Nonrigid Molecules. *Journal of Physical Chemistry A* **2021**, *125*, 4039–4054.

- (363) Chase, M. W.; Curnutt, J. L.; Prophet, H.; McDonald, R. A.; Syverud, A. N. JANAF thermochemical tables, 1975 supplement. *Journal of Physical and Chemical Reference Data* **1975**, *4*, 1–176.
- (364) Yachmenev, A.; Yurchenko, S. N.; Ribeyre, T.; Thiel, W. High-level ab initio potential energy surfaces and vibrational energies of H₂CS. *Journal of Chemical Physics* **2011**, *135*.
- (365) Mardirossian, N.; Head-Gordon, M. Thirty years of density functional theory in computational chemistry: An overview and extensive assessment of 200 density functionals. *Molecular Physics* **2017**, *115*, 2315–2372.
- (366) Goerigk, L.; Hansen, A.; Bauer, C.; Ehrlich, S.; Najibi, A.; Grimme, S. A look at the density functional theory zoo with the advanced GMTKN55 database for general main group thermochemistry, kinetics and noncovalent interactions. *Physical Chemistry Chemical Physics* **2017**, *19*, 32184–32215.
- (367) Hait, D.; Head-Gordon, M. How Accurate Is Density Functional Theory at Predicting Dipole Moments? An Assessment Using a New Database of 200 Benchmark Values. *Journal of Chemical Theory and Computation* **2018**, *14*, 1969–1981.
- (368) Hait, D.; Head-Gordon, M. How accurate are static polarizability predictions from density functional theory? An assessment over 132 species at equilibrium geometry. *Physical Chemistry Chemical Physics* **2018**, *20*, 19800–19810.
- (369) Landrum, G. RDKit: Open-source cheminformatics. 2010; <https://www.rdkit.org/>.
- (370) Biczysko, M.; Panek, P.; Scalmani, G.; Bloino, J.; Barone, V. Harmonic and anharmonic vibrational frequency calculations with the double-hybrid B2PLYP method: Analytic second derivatives and benchmark studies. *Journal of Chemical Theory and Computation* **2010**, *6*, 2115–2125.

- (371) Barone, V.; Biczysko, M.; Bloino, J. Fully anharmonic IR and Raman spectra of medium-size molecular systems: Accuracy and interpretation. *Physical Chemistry Chemical Physics* **2014**, *16*, 1759–1787.
- (372) Barone, V.; Biczysko, M.; Puzzarini, C. Quantum chemistry meets spectroscopy for astrochemistry: Increasing complexity toward prebiotic molecules. *Accounts of Chemical Research* **2015**, *48*, 1413–1422.
- (373) Biczysko, M.; Bloino, J.; Puzzarini, C. Computational challenges in Astrochemistry. *Wiley Interdisciplinary Reviews: Computational Molecular Science* **2018**, *8*, 1349.
- (374) Furtenbacher, T.; Császár, A. G.; Tennyson, J. MARVEL: measured active rotational-vibrational energy levels. *Journal of Molecular Spectroscopy* **2007**, *245*, 115–125.
- (375) Furtenbacher, T.; Császár, A. G. MARVEL: Measured active rotational-vibrational energy levels. II. Algorithmic improvements. *Journal of Quantitative Spectroscopy and Radiative Transfer* **2012**, *113*, 929–935.
- (376) McKemmish, L. K. Molecular diatomic spectroscopy data. *Wiley Interdisciplinary Reviews: Computational Molecular Science* **2021**, *11*, e1520.
- (377) Weser, O. An efficient and general library for the definition and use of internal coordinates in large molecular systems. Ph.D. thesis, Georg August Universität Göttingen, 2017.
- (378) Martin, J. M. L.; Kesharwani, M. K. Assessment of CCSD(T)-F12 Approximations and Basis Sets for Harmonic Vibrational Frequencies. *Journal of Chemical Theory and Computation* **2014**, *10*, 2085–2090.
- (379) Schmitz, G.; Christiansen, O. Accuracy of Frequencies Obtained with the Aid of Explicitly Correlated Wave Function Based Methods. *Journal of Chemical Theory and Computation* **2017**, *13*, 3602–3613.

- (380) Werner, H. J. et al. The Molpro quantum chemistry package. *Journal of Chemical Physics* **2020**, *152*, 144107.
- (381) Halls, M. D.; Velkovski, J.; Schlegel, H. B. Harmonic frequency scaling factors for Hartree-Fock, S-VWN, B-LYP, B3-LYP, B3-PW91 and MP2 with the Sadlej pVTZ electric property basis set. *Theoretical Chemistry Accounts* **2001**, *105*, 413–421.
- (382) Sinha, P.; Boesch, S. E.; Gu, C.; Wheeler, R. A.; Wilson, A. K. Harmonic vibrational frequencies: Scaling factors for HF, B3LYP, and MP2 methods in combination with correlation consistent basis sets. *Journal of Physical Chemistry A* **2004**, *108*, 9213–9217.
- (383) Andersson, M. P.; Uvdal, P. New scale factors for harmonic vibrational frequencies using the B3LYP density functional method with the triple- ζ basis Set 6-311+G(d,p). *Journal of Physical Chemistry A* **2005**, *109*, 2937–2941.
- (384) Merrick, J. P.; Moran, D.; Radom, L. An evaluation of harmonic vibrational frequency scale factors. *Journal of Physical Chemistry A* **2007**, *111*, 11683–11700.
- (385) Andrade, S. G.; Gonçalves, L. C.; Jorge, F. E. Scaling factors for fundamental vibrational frequencies and zero-point energies obtained from HF, MP2, and DFT/DZP and TZP harmonic frequencies. *Journal of Molecular Structure: THEOCHEM* **2008**, *864*, 20–25.
- (386) Laury, M. L.; Boesch, S. E.; Haken, I.; Sinha, P.; Wheeler, R. A.; Wilson, A. K. Harmonic Vibrational Frequencies: Scale Factors for Pure, Hybrid, Hybrid Meta, and Double-Hybrid Functionals in Conjunction with Correlation Consistent Basis Sets. *Journal of computational chemistry* **2011**, *32*, 2339–2347.
- (387) Laury, M. L.; Carlson, M. J.; Wilson, A. K. Vibrational frequency scale factors for density functional theory and the polarization consistent basis sets. *Journal of Computational Chemistry* **2012**, *33*, 2380–2387.

- (388) Chan, B.; Radom, L. Frequency Scale Factors for Some Double-Hybrid Density Functional Theory Procedures: Accurate Thermochemical Components for High-Level Composite Protocols. *Journal of Chemical Theory and Computation* **2016**, *12*, 3774–3780.
- (389) Chan, B. Use of Low-Cost Quantum Chemistry Procedures for Geometry Optimization and Vibrational Frequency Calculations: Determination of Frequency Scale Factors and Application to Reactions of Large Systems. *Journal of Chemical Theory and Computation* **2017**, *13*, 6052–6060.
- (390) Pulay, P.; Fogarasi, G.; Pongor, G.; Boggs, J. E.; Vargha, A. Combination of Theoretical ab Initio and Experimental Information to Obtain Reliable Harmonic Force Constants. Scaled Quantum Mechanical (SQM) Force Fields for Glyoxal, Acrolein, Butadiene, Formaldehyde, and Ethylene. *Journal of the American Chemical Society* **1983**, *105*, 7037–7047.
- (391) Rauhut, G.; Pulay, P. Transferable scaling factors for density functional derived vibrational force fields. *Journal of Physical Chemistry* **1995**, *99*, 3093–3100.
- (392) Baker, J.; Jarzecki, A. A.; Pulay, P. Direct scaling of primitive valence force constants: An alternative approach to scaled quantum mechanical force fields. *Journal of Physical Chemistry A* **1998**, *102*, 1412–1424.
- (393) Fekete, Z. A.; Hoffmann, E. A.; Kortvlyesi, T.; Penke, B. Harmonic vibrational frequency scaling factors for the new NDDO Hamiltonians: RM1 and PM6. *Molecular Physics* **2007**, *105*, 2597–2605.
- (394) Borowski, P.; Fernández-Gómez, M.; Fernández-Liencres, M. P.; Ruiz, T. P. An effective scaling frequency factor method for scaling of harmonic vibrational frequencies: theory and preliminary application to toluene. *Chemical Physics Letters* **2007**, *446*, 191–198.
- (395) Borowski, P.; Drzewiecka, A.; Fernández-Gómez, M.; Fernández-Liencres, M. P.; Ruiz, T. P. An effective scaling frequency factor method for harmonic vibrational frequencies: The factors' transferability problem. *Chemical Physics Letters* **2008**, *465*, 290–294.

- (396) Borowski, P. An effective scaling frequency factor method for scaling of harmonic vibrational frequencies: The use of redundant primitive coordinates. *Journal of Molecular Spectroscopy* **2010**, *264*, 66–74.
- (397) Borowski, P.; Drzewiecka, A.; Fernández-Gómez, M.; Fernández-Liencres, M. P.; Ruiz, T. P. A new, reduced set of scaling factors for both SQM and ESFF calculations. *Vibrational Spectroscopy* **2010**, *52*, 16–21.
- (398) Brittain, D. R.; Lin, C. Y.; Gilbert, A. T.; Izgorodina, E. I.; Gill, P. M.; Coote, M. L. The role of exchange in systematic DFT errors for some organic reactions. *Physical Chemistry Chemical Physics* **2009**, *11*, 1138–1142.
- (399) Tentscher, P. R.; Arey, J. S. Geometries and vibrational frequencies of small radicals: Performance of coupled cluster and more approximate methods. *Journal of Chemical Theory and Computation* **2012**, *8*, 2165–2179.
- (400) Yu, H.; Truhlar, D. G. Components of the Bond Energy in Polar Diatomic Molecules, Radicals, and Ions Formed by Group-1 and Group-2 Metal Atoms. *Journal of Chemical Theory and Computation* **2015**, *11*, 2968–2983.
- (401) Yu, H. S.; Li, S. L.; Truhlar, D. G. Perspective: Kohn-Sham density functional theory descending a staircase. *Journal of Chemical Physics* **2016**, *145*, 130901.
- (402) Hsu, Y.-C. Bending Vibrational Levels in the Electronic Spectra of Small Radicals. *Journal of the Chinese Chemical Society* **2018**, *65*, 395–404.
- (403) Tew, D. P.; Klopper, W.; Heckert, M.; Gauss, J. Basis set limit CCSD(T) harmonic vibrational frequencies. *Journal of Physical Chemistry A* **2007**, *111*, 11242–11248.